NACA
TN
2962
c. 1

9275

NACA TN 2962

TECH LIBRARY KAFB, NM
0065942

NATIONAL ADVISORY COMMITTEE FOR AERONAUTICS

TECHNICAL NOTE 2962

EFFECT OF ICE AND FROST FORMATIONS ON DRAG OF NACA 65_1-212 AIRFOIL FOR VARIOUS MODES OF THERMAL ICE PROTECTION

By Vernon H. Gray and Uwe H. von Glahn

Lewis Flight Propulsion Laboratory
Cleveland, Ohio

LOAN COPY: RETURN TO
AFWL-SUL
KIRTLAND AFB, N. M.

Washington
June 1953

AFMDC
TECHNICAL LIBRARY
AFL 2811

TECH LIBRARY KAFB, NM
0065942

1E

NATIONAL ADVISORY COMMITTEE FOR AERONAUTICS

TECHNICAL NOTE 2962

EFFECT OF ICE AND FROST FORMATIONS ON DRAG OF NACA 65_1-212 AIRFOIL FOR VARIOUS MODES OF THERMAL ICE PROTECTION

2744

By Vernon H. Gray and Uwe H. von Glahn

SUMMARY

The effects of primary and runback icing and frost formations on the drag of an 8-foot-chord NACA 65_1-212 airfoil section were investigated over a range of angles of attack from 2° to 8° and airspeeds up to 260 miles per hour for icing conditions with liquid-water contents ranging from 0.25 to 1.4 grams per cubic meter and datum air temperatures of -30° to 30° F.

The results showed that glaze-ice formations, either primary or runback, on the upper surface near the leading edge of the airfiol caused large and rapid increases in drag, especially at datum air temperatures approaching 32° F and in the presence of high rates of water catch. Ice formations at lower temperatures (rime ice) did not appreciably increase the drag coefficient over the initial (standard roughness) drag coefficient. Cyclic de-icing of the primary ice formations on the airfoil leading-edge section permitted the drag coefficient to return almost to the bare airfoil drag value. Runback icing on the lower surface did not present a serious drag problem except when heavy spanwise ridges of runback ice occurred aft of the heatable area. Frost formations caused rapid and large increases in drag with incipient stalling of the airfoil.

1-HC

INTRODUCTION

One of the most important problems associated with aircraft icing is the effect of various-shaped ice formations on the performance of the aircraft, specifically the effects of ice and frost formations on lift and drag characteristics of airfoils. Establishment of these effects will help determine (1) the design requirements of icing-protection systems currently being developed and (2) the necessity for means of preventing the accumulation of frost on aircraft surfaces prior to and during take-off.

A study of the icing-protection requirements for high-speed, high-altitude, turbojet-powered aircraft (ref. 1) indicates that continuous heating systems for airfoils, designed to evaporate all the impinging

water for selected meteorological icing conditions, will result in prohibitive loads on the available heat sources and large deterioration of aircraft performance. As a means for reducing these high heat loads, cyclic de-icing systems (refs. 2 and 3) have been proposed. Cyclic de-icing systems, however, are subject to runback icing on the surfaces aft of the heated areas (due to melting of some ice during the heating period) and considerable leading-edge icing during the heat-off period. The effects of ice formations on airfoil characteristics were insufficiently established to permit an evaluation in reference 1 of the reduction in aerodynamic performance of aircraft equipped with cyclic de-icing systems.

2744

An evaluation of the effect of runback ice formations on airfoil characteristics is also of interest for continuous heating systems. In general, a continuous heating system is designed to evaporate the impinging water for a particular icing condition; and if a more severe icing condition is encountered, some water will not be evaporated, with a consequent formation of runback icing. Furthermore, it is pointed out in reference 1 that a considerable saving in heat can be accomplished for a continuous heating system if some runback icing can be tolerated for a selected design meteorological icing condition. It is of interest, therefore, to ascertain whether the drag resulting from runback icing is more detrimental to performance than is the propulsion penalty incurred by supplying the additional heat necessary to evaporate all the impinging water.

The problem of frost formations on aircraft is also of increasing importance in cold climates. These aircraft are subject to heavy ground frost formations over most of the exposed surfaces; and, if they are provided with a conventional wing anti-icing system, removal of frost is generally limited to the heatable areas which extend usually from the zero chord point to less than 20 percent of chord. The seriousness of the problem must be established in order that the necessity for removing all or part of such frost formations before take-off be understood.

In previous experimental studies, particularly those reported in reference 4, the effect of protuberances on airfoil characteristics was investigated; however, these studies used spoilers mounted perpendicularly to the airfoil surface or smoothly faired protuberances rather than the irregular and rough surfaces associated with ice formations. An effort was made in reference 5 to simulate ice formations by means of tar, slag, and asphalt. These formations did not truly represent natural ice formations, although the aerodynamic characteristics exhibited by the airfoil used in this study gave an indication of the serious aerodynamic problems caused by ice formations.

The NACA Lewis laboratory is investigating experimentally the effect of these frost and ice formations on airfoil drag characteristics. Studies have been conducted to relate size, shape, and type of various

frost and ice formations to changes in the drag of an airfoil section. These studies include investigations with an airfoil having its leading-edge section unheated, continuously heated, and cyclically heated for de-icing. In addition, the portion of the airfoil aft of 12 percent of chord has been heated continuously and also unheated to determine the effect on airfoil drag of frost formations on this portion of the wing. The change in airfoil drag as a function of duration in icing for various icing conditions was also investigated.

The results presented herein were obtained with an 8-foot-chord NACA 65_1-212 airfoil model employing a hot-gas icing-protection system (ref. 2). The airfoil study was conducted over the following range of icing and operating conditions:

Angle of attack, deg	2 to 8
Airspeed, mph	100 to 260
Liquid-water content, g/cu m	0.25 to 1.4
Datum air temperature, $^{\circ}F$	-30 to 30
Mean effective droplet size, microns	10 to 16

APPARATUS AND INSTRUMENTATION

The model used in this study (and that of ref. 2) is an NACA 65_1-212 airfoil section of 8-foot chord spanning the 6-foot height of the Lewis icing research tunnel. The airfoil leading-edge section, consisting of three spanwise segments, may be gas-heated by means of chordwise passages to 12 percent of chord. The center segment is 3 feet in span, and the top and bottom segments are 1.5 feet each in span (fig. 1). All segments were capable of being heated independently for cyclic ice removal or collectively for continuous heating. For the cyclic de-icing studies a continuously heated spanwise parting strip was used near the zero chord line (ref. 2).

Aft of 12 percent of chord the model was divided into four compartments (fig. 1), each capable of being individually heated by means of steam. The inside of each compartment was lined with 1/16-inch-thick neoprene to reduce the surface temperature, which otherwise might have resulted in sufficient heat transfer to the airfoil wake to affect the drag measurements. In order to prevent steam leakage into the wake, these compartments (hereinafter designated afterbody) were operated under a slight vacuum.

As an aid in estimating the chordwise extent of ice and frost formations, 1/2-inch squares, spaced 1/2 inch apart, were painted on the airfoil surfaces.

A pressure rake located 1/4 chord behind the trailing edge of the airfoil (fig. 1) was used to measure the airfoil drag. The rake consisted of 71 electrically heated total-pressure tubes and 9 static-pressure tubes. All the tubes were spaced on 1/4-inch centers. The supports for the rake were air-heated for icing protection.

EXPERIMENTAL CONDITIONS AND TECHNIQUES

For convenience in evaluating the effect of ice formations on the drag of an airfoil, the following modes of heating were employed:

Leading-edge section	Afterbody	Desired drag information
Unheated	Unheated	Combined effect of frost and ice deposits
	Heated	Effect of ice formation
Continuously heated	Unheated	Combined effect of frost and runback ice deposits
	Heated	Effect of runback icing
Intermittently heated	Unheated	Combined effect of frost and ice deposits
	Heated	Effect of primary ice deposits and runback icing

For studies requiring heating of the leading-edge section, the results of reference 2 establishing the heating quantities necessary for adequate icing protection at selected meteorological icing conditions were used in the initial test conditions. Changes in these quantities were then made, as required, in order to obtain specifically desired types or formations of ice on the airfoil surfaces. In general, the rearward three steam-heated compartments were heated as a unit, and runback icing was allowed to form only on the first compartment behind the leading-edge section. For studies in which the leading-edge section was unheated and the afterbody steam-heated, all four compartments were heated together. The range of conditions covered in these studies was as follows: airspeed, 180 and 260 miles per hour; water content, 0.25 to 1.4 grams per cubic meter; and datum air temperature, 0° to 30° F.

2744

The angles of attack included in the investigation were 2°, 5°, and 8°. In addition, ice formations were allowed to build up on the leading edge at a low angle of attack (2° or 5°) for a period of about 4 minutes and the angle then changed to 8°. This procedure permitted a measurement of the drag produced by icing that might be encountered with a cyclic de-icing system during the heat-off period in an airplane letting down through an icing cloud and then flaring out for a landing approach.

2744

Similar studies were made with the leading-edge section continuously heated but with some runback icing permitted to form on the airfoil surfaces aft of the heated leading-edge section to determine the effect of runback icing.

Datum air temperature was defined and determined as the average surface temperature of the unheated airfoil leading-edge section. In icing conditions, the datum temperature was determined from thermocouples that were shielded from or not subject to the fusion of impinged water. For the range of conditions investigated, little difference between datum and total air temperature was found. The icing conditions were determined from a previous calibration of the tunnel and periodically checked with a pressure-type icing-rate meter (ref. 6). The mean effective droplet size in these studies ranged from 10 to 16 microns as determined from a dye-tracer technique.

Because the tunnel airspeed was limited to 260 miles per hour, rates of icing and ice formations associated with higher speeds were obtained by increasing the liquid-water contents considerably above generally accepted values for natural icing clouds with the air temperatures used in the studies. In the absence of exact knowledge on droplet-impingement characteristics of the test airfoil, the data are discussed in general terms of water catch, defined in this investigation as a function only of liquid-water content and airspeed, rather than the more complex function requiring airfoil collection efficiency based on droplet size. By this means, the size of the ice formations obtained at airspeeds used in this investigation and at high liquid-water contents may be assumed to be approximately representative of ice formations at twice the airspeed and half the liquid-water content.

For studies of the effect of afterbody frost formations on the drag of the airfoil, no heat was furnished to the afterbody. Frost formed on the afterbody because of air-stream turbulence and the supersaturated condition of the tunnel air. The studies with frost on the afterbody only were made over the same range of conditions as the icing studies. For studies in which the leading-edge section as well as the afterbody was coated with a frost formation, the tunnel air was refrigerated to -30° F, after which refrigeration was turned off and the ventilating doors of the tunnel were opened to permit warm moist air to pass over

the cold model. Moisture condensing on the model from this warmer air soon covered the model with a fine coat of frost. Drag measurements with the pressure rake were made throughout the test. The frost studies with a fully frosted airfoil were made at an angle of attack of 8° and at a speed of about 100 miles per hour, simulating take-off conditions.

Throughout the investigations, photographs of ice and frost formations were taken to correlate the size and shape of these formations with the changes in drag as determined with the pressure rake.

2744

RESULTS AND DISCUSSION

Evaluation of the data obtained in this study of the effect of various icing formations is presented in terms of the general increase in drag with duration in icing as well as with specific ice formations permitted to form at particular locations on the airfoil. After presentation of the drag data obtained in the investigation, a brief discussion of the significance of the results is presented.

The investigation of the airfoil drag studies reported herein is divided into two primary categories. The first category is concerned with the increase in drag caused by ice formations associated with various modes of supplying heat to the leading-edge section; and the second, with an evaluation of the effect on airfoil drag of frost formations with and without accompanying ice formations. Tunnel wall interference effects were not evaluated.

Three general types of leading-edge ice formations were investigated (fig. 2). The first, a rime-ice formation (fig. 2(a)), was associated with a datum air temperature of 0° F and was essentially independent of liquid-water content. These ice formations conformed closely to the airfoil contour and faired generally forward into the air stream. The second type, a glaze-ice formation (fig. 2(b)), was obtained with a datum air temperature of approximately 25° F and relatively low rates of water catch. These ice formations generally built outward at an angle to the air stream, but the primary ice formation was still somewhat faired into the airfoil contour and did not penetrate excessively into the flow field near the stagnation region. The final type, a rough, angular, glaze-ice formation (fig. 2(c)), was obtained at datum air temperatures of about 30° F at moderate rates of water catch and at air temperatures down to 25° F with high rates of water catch. This glaze ice, especially near the stagnation region, formed a double-peaked mushroom shape. The growth of the ice formation was approximately normal to the airfoil surface, with the peaks jutting abruptly into the flow field and causing a flow disturbance, especially at high angles of attack. These glaze-ice formations may be associated with combinations of flight speed, liquid-water content, and ambient-air temperature; consequently, they can occur at low altitude under conditions of low airspeed in icing clouds of high

ambient-air temperature, or at high altitudes under conditions of high speed and low ambient-air temperature. In the latter case, the release of the heat of fusion and the aerodynamic heating of the airfoil surfaces combine to promote the formation of glaze ice.

A brief study of the effect of a water film at above-freezing temperatures on airfoil drag characteristics was also conducted. The water-film effect on drag at low angles of attack was negligible. At high angles of attack (8°) an increase of as much as 15 percent in the drag coefficient was obtained with a high rate of water catch. This value was, however, within the range of drag change caused by normal roughening of the airfoil surfaces by foreign particles in the tunnel air stream.

2744

Effect of Ice Formations on Airfoil Drag

Leading-edge section unheated. - The drag measurements indicated that when ice was permitted to collect on an unheated airfoil model at a low rate of water catch only small increases in drag occurred during an icing period of 30 minutes (fig. 3). The drag coefficient increased by about 6 percent during the initial 3 minutes of icing, and thereafter a more gradual increase in drag occurred. The primary ice formations blended smoothly into the flow field about the airfoil, and disruptions in the boundary layer that cause large drag increases were avoided. The feather-type ice formations pointing forward into the air stream behind the first 3 inches of primary icing on the leading-edge section were sufficiently streamlined and faired into the general flow field (see also figs. 2(a) and (b)) to avoid any excessive contributions to an increase in drag. The largest increases in drag coefficient with time occurred at an angle of attack of 5°. The maximum increase, 0.00375 or 40 percent, occurred at a 5° angle of attack and a datum air temperature of 25° F after 20 minutes of icing; however, part of this ice formation subsequently broke off with a resultant decrease in drag coefficient. For all the icing conditions illustrated in figure 3, the increase in drag coefficient following a 30-minute icing period was less than 27 percent. In conjunction with the drag values shown in figure 3, a sequence of photographs showing the progressive build-up of ice formations at a datum air temperature of 0° F together with corresponding drag coefficients is shown in figures 4, 5, and 6 for angles of attack of 2°, 5°, and 8°, respectively. A similar sequence of photographs taken for an icing condition at a datum air temperature of 25° F is shown in figures 7 and 8 for angles of attack of 5° and 8°, respectively.

The effect on drag of mushroom-type ice formations associated with icing at datum air temperatures near the freezing point, discussed in conjunction with figure 2(c), is illustrated in figure 9. At an angle of attack of 8° the protrusion of the leading-edge ice formation into

the flow field caused an increase in drag coefficient from 0.0128 to 0.0222 after 28 minutes. This increase in drag was accompanied by a shift in the momentum wake toward the upper surface, which indicated a possible loss in lift. Subsequent blow-off of a portion of the upper-surface ice formation (fig. 9(b)) resulted in a sharp decrease in drag coefficient to 0.0153. It is apparent, therefore, that the ice formations on the upper surface near the leading edge of an airfoil have the greatest effect on drag. The shift of the momentum wake back in the direction of the lower surface as the ice blew off indicated that the upper-surface leading-edge ice formation was also responsible for the apparent changes in lift.

2744

Another example of a mushroom-type ice formation on the airfoil leading edge is shown in figure 9(c) for a 5° angle of attack. The magnitude of the drag-coefficient increase is comparable to that obtained at an 8° angle of attack; however, no particular shift in momentum wake indicative of a loss in lift was observed.

Leading-edge section continuously heated. - The data presented in this section are particularly applicable to anti-icing systems that do not evaporate all the impinging water, but allow runback icing (fig. 10). Such runback icing may be encountered when an anti-icing system is thermally submarginal for the icing condition encountered. On the basis of the heating rates established for continuously heating the leading-edge section in reference 7, the heating rates used herein were about 28 to 45 percent of those necessary for total evaporation of the impinging water. The percentage of the total amount of water impinging on the airfoil that was evaporated by the heating rates given in figure 10 would be approximately of the same magnitude (ref. 1).

The drag-coefficient changes caused by such runback icing are primarily functions of the rate of water catch, heating rate, and datum air temperature. All three factors contribute to the size, location, and shape of the runback ice formations and consequently to the drag of the airfoil. From the drag-coefficient changes shown in figure 10, the drag appears to increase more rapidly with time in icing at a high datum air temperature than at a low datum air temperature, as a result of the bulkier and generally rougher ice usually associated with high datum air temperatures.

The increase in drag coefficient at a 2° angle of attack with time in an icing condition is shown in figure 10 with the corresponding photographs of the runback icing shown in figure 11. The data shown are for a high rate of water catch at a datum air temperature of 0° F. The drag coefficient increased 29 percent in 20 minutes of icing with most of the runback ice formation located near 13 percent of chord. Some small runback icing streaks on the upper surface may be observed at about 8 percent of chord in figure 11(d), with two V-shaped formations just above

the center of the airfoil span. Although the datum air temperature was low in this study, the runback icing was of a glaze-type ice structure, with rime-ice deposits occurring only as the result of direct droplet impingement on the residual runback icing. On the lower surface the runback icing extended from about 13 to 20 percent of chord (figs. 11(a) and (c)). The runback formations on the upper surface were generally shorter than those on the lower surface. After 20 minutes of icing at a 2° angle of attack, the angle was changed to 8° to simulate a landing-approach condition with the ice shown in figure 11(d) still on the airfoil. Only a small increase in drag coefficient over the bare airfoil drag at the 8° angle of attack was observed that could be attributed to these runback ice formations (fig. 10).

2744

At a 5° angle of attack an increase in drag coefficient of approximately 39 percent was obtained in $14\frac{1}{2}$ minutes of icing (fig. 10) with a relatively low rate of water catch and a datum air temperature of 25° F. Photographs of the runback ice formations associated with this drag increase are shown in figure 12. A spanwise ice ridge accummulated on the lower surface at approximately 13 percent of chord, while a series of runback patches formed on the upper surface. The formation on the lower surface was not caused by runback icing alone, but also by direct water impingement as the ice formation began to protrude into the air stream. A comparison of figures 12(a) and 12(c) shows that, on the upper surface, only the runback ice formations near the leading edge show an appreciable increase in size in 8 minutes of icing; the increase in drag coefficient is apparently caused primarily by the spanwise ridge-ice formation on the lower surface. At a datum temperature of 0° F with low rates of water catch, the drag coefficient at an angle of attack of 5° did not change appreciably with time in icing (fig. 10). For these conditions, the airfoil drag coefficients with submarginal heating of the leading-edge section are nearly the same as those for comparable conditions with no leading-edge heating.

2-HC

At an 8° angle of attack the physical dimensions and locations of runback icing have a pronounced effect on the drag coefficient (fig. 10). As the heating rate is decreased or as the rate of water catch is increased, the drag coefficient increases correspondingly. The effect on drag coefficient of a reduction in heat supply of 23 percent from 5850 Btu/(hr)(ft span) to the leading-edge section for a given icing condition is shown in figure 10 for an 8° angle of attack and a datum air temperature of 25° F. At the reduced heating rate of 4500 Btu/(hr)(ft span), a 10-percent increase in drag occurred in the initial 2 minutes of icing; thereafter the drag coefficient increased at approximately the same rate as with the higher heat flow. The use of a lower heating rate caused a forward movement of runback ice formations as well as slightly larger ice formations because of the evaporation of less water in the heated area.

For the runback ice formation shown in figures 13(a) and (b) the drag coefficient was increased only 12 percent after $15\frac{1}{2}$ minutes of icing. From the appearance and location of the icing, it is seen that most of this increase in drag was caused by the lower-surface icing. After an additional $6\frac{1}{2}$ minutes of icing (fig. 13(c)) the drag coefficient had not increased appreciably, primarily because the spanwise ice ridge shed intermittently in small chunks and thereby prevented a large increase in the total amount of runback ice accumulation.

2744

A photograph of a heavy runback ice formation on the upper surface near the airfoil leading edge at an 8° angle of attack is shown in figure 14(a). The accompanying spanwise ice ridge caused by runback icing on the lower surface is shown in figure 14(b). These ice formations occurred at a datum air temperature of 25° F and a relatively low liquid-water content for 22 minutes of icing, after which a high liquid-water content was obtained for 7 more minutes. The drag coefficient of 0.0217 is 67 percent higher than the bare airfoil drag value and was accompanied by a pronounced shift in the momentum wake, which indicated incipient stalling of the airfoil. Removal of the patches of runback icing on the upper surface to a distance about 12 percent of chord behind the leading edge (fig. 14(c)) resulted in a reduction of the drag coefficient to 0.0175 (35 percent above bare airfoil drag), although the lower-surface ice ridge was substantially unchanged. The majority of this remaining drag can probably be attributed to the ridge of runback icing on the lower surface, as was indicated for figure 13.

Leading-edge section cyclically de-iced. - For a cyclically de-iced leading-edge section, the change in drag coefficient caused by leading-edge icing during the heat-off period and runback icing during the heat-on period is shown in figure 15 as a function of icing time; all the icing conditions shown in figure 15 resulted in the relatively small, generally streamlined ice formations shown in figures 2(a) and (b). The curves in figure 15 indicate that only a gradual increase in drag occurs for icing times up to 50-minutes duration. The drag coefficient at all angles of attack studied increased a maximum of 0.0012 (10 percent) during a 4-minute heat-off period with a datum air temperature of 25° F. After the heating period the drag coefficient generally approached within 5 percent of the initial bare airfoil drag value. Practically no increase in drag was obtained at a datum air temperature of 0° F. At a datum air temperature of 0° F, permitting the airfoil to ice at a low angle of attack (2° or 5°) during a 4-minute heat-off period and then increasing the angle of attack to 8°, to simulate a landing approach, increased the drag coefficient by approximately 18 percent over the drag value associated with a 4-minute icing period at the high angle of attack; however, upon ice removal the drag coefficient nearly approached the bare airfoil drag value. An increase in the liquid-water content to

obtain a high rate of water catch did not significantly increase the drag coefficient at a 2° angle of attack and a datum air temperature of 0° F.

Photographs illustrating the type and magnitude of typical leading-edge icing and residual icing following the heating period are shown in figures 16 to 19 and apply to the drag data shown in figure 15. Increasing the heat-off period from 4 to 12 minutes with a low rate of water catch at a datum air temperature of 0° F did not appreciably change the drag coefficient (fig. 15), although the ice formations accumulated in the longer icing period were considerably larger (fig. 18(c)). The use of a parting strip with a cyclic de-icing system at low rates of water catch had no apparent effect on the airfoil drag during the icing period when compared with an unheated leading-edge section (see figs. 3 and 15).

For conditions that produced mushroom-type glaze-ice formations (high liquid-water content and high datum air temperature), rapid and large drag increases were incurred during 4-minute icing periods (fig. 20). At 2° angle of attack the drag coefficient increased by as much as 0.0061 (59 percent) during a 4-minute icing period. With an 8°-angle-of-attack attitude, the drag coefficient increased by as much as 0.0089 (68 percent) during the initial 2 minutes of a heat-off period and as much as 0.0093 (71 percent) for the full 4-minute heat-off period. At 5° angle of attack, the rate of increase of the drag coefficient with icing time was not as rapid as at 2° and 8° angles of attack, because the rate of water catch was lower. The largest percentage of drag increase during a heat-off period at 5° angle of attack was about 22 percent, except for the initial cycle.

The effect of a gradual increase in residual runback icing with icing time on drag coefficient is illustrated in figure 21. After approximately 9 minutes in icing at an angle of attack of 2°, the drag coefficient before ice removal reached a value of 0.0142 and returned to 0.00973 after ice was shed (figs. 21(a) and (b)). After approximately 23 minutes in icing, the drag coefficient reached a value of 0.0164 before ice removal and returned to a value 0.0114 after removal (figs. 21(c) and (d)). The cause for the increase with time of the drag coefficient after ice removal is apparent from the larger ice formations remaining on the lower surface after 23 minutes in icing. The growth of these ice formations may be greatly limited by the use of a secondary cycling arrangement. With this procedure, the de-icing system is operated for several cycles so that runback ice forms on the rear portion of the heatable area. Then, on a subsequent cycle, a higher heating rate or longer heating time is used, which allows the rear surface areas to heat up more than previously and thereby remove the runback ice. Although some runback icing will occur on unheatable areas during the secondary cycles, repetition of this heating pattern will greatly decrease the permanent runback ice formations.

2744

CH-2 back

Additional photographs of typical ice formations obtained on the airfoil under conditions of high rates of water catch and a datum air temperature of approximately 25° F together with the associated drag coefficients are shown in figures 22 and 23. In most cases, a drag coefficient on the order of 0.020 at an angle of attack of 8° was accompanied by a marked shift of the momentum wake behind the airfoil toward the upper airfoil surface, which indicated a loss in lift and approach of stall for the airfoil. These shifts of the wake often occurred within 90 seconds after the start of a heat-off or icing period. A study of the drag-coefficient changes associated with the icing photographs of figure 24 again indicates that the high drag value is caused by the upper-surface icing at the leading edge. The large residual or runback ice formations on the lower surface, together with runback on the upper surface 6 inches behind the leading edge, contribute only an increase of about 0.0032 (26 percent) to the drag coefficient; whereas the ice formed at the leading edge during the heat-off period contributes an additional increase to the drag coefficient of about 0.0084 or a total drag increase of about 96 percent. The shift observed in momentum wake behind the airfoil was caused by the upper-surface leading-edge ice formation. The drag value after several cycles of ice removal showed an increase over the bare airfoil drag of about the same order as runback icing discussed in the section on continuous heating.

2744

A decrease in the heat flow to the leading-edge section and an increase in the heating time had no appreciable effect on the drag coefficient. The runback icing incurred by changes in cycle timing is apparently in the same category as runback icing incurred with a continuously heated system that does not evaporate all the impinging water; hence, only small increases in drag are obtained.

The drag associated with ice accumulated during a heat-off or icing period at a datum air temperature of 25° F during three simulated landing-approach procedures was studied. The data obtained are shown in figure 25. The drag coefficient for approach condition A (see legend in fig. 25 for conditions) increased from 0.0088 to 0.0393 (347-percent increase) as the angle of attack was changed from 2° to 8°. Following cyclic operation of the icing-protection system the drag coefficient was reduced to within 20 percent of the bare airfoil drag coefficient at 8° angle of attack. At a high rate of water catch (condition B) the drag coefficient for a simulated approach increased from 0.0123 to 0.0502 (308-percent increase) when the angle of attack was changed from 2° to 8° near the end of a 4-minute icing period. This is an increase of 509 percent over the bare airfoil drag at a 2° angle of attack and 285 percent over the bare airfoil drag at 8° angle of attack. Similarly, changing the angle of attack from 5° to 8° (condition C) increased the drag coefficient from 0.0113 to 0.027 (139 percent). Upon removal of this ice formation during the heating period, the drag coefficient returned to within 5 percent of the bare airfoil drag at 8° angle of attack. These large drag increases were caused by the ice formation just

aft of the leading edge on the upper surface of the airfoil and were accompanied by a stalling characteristic of the airfoil. The number of cycles at the low angles of attack does not appreciably affect the sharp rise in drag as the angle of attack is increased to 8°; however, the residual runback icing formed during cycles at low angles of attack will determine how closely the drag after an angle-of-attack change to 8° will approach the bare wing drag at 8° angle of attack following the heat-on period.

2744

General comments on effect of icing on airfoil drag. - In general, the studies showed that primary ice formations incurred near the air stagnation region on the upper surface of an airfoil at high datum air or surface temperatures in the presence of a high rate of water catch cause a severe and often prohibitive increase in drag, especially at high angles of attack. From the data presented herein it is apparent that ridges or heavy accretions of runback ice formations on the upper surface near the zero chord point are detrimental to airfoil aerodynamic characteristics at high angles of attack. Spanwise ridges of heavy runback icing on the lower surface may cause appreciable drag increases at low angles of attack. Chordwise streaks of runback icing away from the leading edge on either surface of the airfoil do not appear to cause significant changes in airfoil drag.

A comparison of the effect of runback icing incurred with a continuously heated leading-edge section that does not evaporate all the impinging water with one that is cyclically de-iced (figs. 10 and 20, respectively) shows that in a severe icing condition (datum air temperature, 25° F; angle of attack, 8°; airspeed, 260 mph; and a water content of approximately 1.0 g/cu m) the drag coefficient with continuous heating increased to a value of 0.018 in 12 minutes, whereas the maximum value after de-icing with a cyclic system did not exceed 0.016 in 28 minutes. The slope of the drag-coefficient curve for continuous heating indicates that for a similar 28-minute icing period the drag coefficient could have reached a value of about 0.024, an increase in total drag due to runback icing of 50 percent over the cyclically de-iced airfoil. For low rates of water catch (figs. 10 and 15), the drag increases incurred with a continuously heated leading-edge section that allows some runback icing to occur are about the same as the drag incurred with runback icing for a cyclically de-iced airfoil.

Glaze-ice formations on the leading-edge section during a simulated approach cause a severe increase in drag coefficient and are accompanied by a shift in the position of the momentum wake, which indicates incipient stalling of the airfoil.

Effect of Surface Frost on Drag Characteristics

Unpublished NACA data indicate that frost deposits on the surface of an airfoil afterbody behind the heated leading-edge section have a great effect on the airfoil drag characteristics. An effort was made to evaluate this effect quantitatively by applying several grades of sandpaper to specific areas of the afterbody and to study the effect of this roughness on airfoil drag values. With both airfoil surfaces covered symmetrically with fine grade, 120-grit sandpaper aft of 20 percent of chord, an almost linear rise in drag coefficient as a function of the airfoil surface covered was noted over a range of angles of attack from 0° to 8°. This increase in drag coefficient amounted to 0.00005 per percent of the total surface covered. It was also observed that applying sandpaper to the lower surface alone contributed only about 25 percent of the total increase in drag obtained with sandpaper on both upper and lower surfaces.

2744

The afterbody frost formations obtained in icing tunnels are believed to be caused by turbulence of the air stream, which deposits minute droplets on the surfaces, and by a condition of supersaturation, which promotes the growth of frost deposits. The initial frost deposit on an afterbody appears immediately upon starting a spray cloud through the tunnel and takes the form of a latticework of pinhead size crystalline deposits on both upper and lower surfaces of the airfoil (fig. 26(a)). As the frost formation increases in size with time in the icing condition, water droplets begin to impinge directly on the frost pinnacles (fig. 26(b)). The deposition of droplets on the frost pinnacles causes small featherlike formations composed of ice and frost particles to grow forward into the air stream (fig. 26(c)). These feathers increase in size and may reach a length of several inches and protrude as much as 1 inch in a direction normal to the air stream (fig. 26(d)).

In order to illustrate the increase in drag that may occur from frost formations on an airfoil, the following sections discuss the drag changes obtained in combination with leading-edge icing and several modes of removing the leading-edge icing while permitting the frost formations to remain on the afterbody surfaces. Such combinations of circumstance may be encountered in flight during a change from cold to warmer, more humid icing conditions and in a take-off in cold weather conditions conducive to frost formations on aircraft surfaces.

Leading-edge section unheated. - The combination of leading-edge ice formations and frost on the afterbody surfaces causes a rapid and large increase in airfoil drag (fig. 27) for icing periods up to 32-minutes duration. At a 5° angle of attack and approximately equal water-catch rates, a change in datum air temperature from 0° to 22° F did not

materially affect the rate of change in the drag coefficient. For these conditions the drag coefficient was increased by about 100 percent after 25 minutes of icing. At an angle of attack of 8° the rate of change of the drag coefficient with time in icing was approximately the same as at a 5° angle of attack. An increase in liquid-water content from 0.53 to 1.4 grams per cubic meter, resulting in a higher total water-catch rate and an increased frost-deposit rate, increased the rate of change of the drag coefficient, the drag increasing by 100 percent after only $7\frac{1}{2}$ minutes. The rapid rise in drag for this condition is due in great part to the heavy glaze mushroom-ice formation on the leading edge (fig. 28). A sequence of additional photographs illustrating the ice and frost formations that caused the drag changes presented in figure 27 are shown in figures 29 and 30. A comparison of figures 6(a) and 6(b) with figures 30(a) and 30(b), respectively, indicates that the leading-edge ice formations are quite similar; the difference in drag coefficient (36 percent after 21 min) can, therefore, be attributed to the afterbody frost formations.

2744

Leading-edge section continuously heated. - Continuously heating the leading-edge section and permitting frost to accummulate on the afterbody can result in an extremely rapid initial increase in drag coefficient at high rates of water catch (fig. 31). Such a condition may be encountered during take-off and climb in cold climates. At an angle of attack of 2° with a high rate of water catch, an increase in drag coefficient from 0.00785 to 0.0132 (68 percent) occurred within 1 minute after icing started. Photographs of the frost formations on the afterbody indicate that the initial drag increase was caused by small pinhead frost deposits on both upper and lower surfaces of the airfoil similar to the frost shown in figure 26(a). At the end of 25 minutes in the same icing condition, the drag coefficient had reached 0.0235, an increase of almost 200 percent over the bare airfoil drag value. Photographs of this icing condition (fig. 32) indicate runback icing similar to that shown in figure 11 in addition to the afterbody frost. For an icing period of 15 minutes, the drag coefficient was about 70 percent greater with frost than without frost formations on the afterbody. It is apparent that the difference in drag values again is caused by the afterbody frost formations. After 25 minutes in the icing condition at an angle of 2°, the angle of attack was changed to 8° with a consequent rise in drag coefficient from 0.0235 to 0.0274 (fig. 31). Although the afterbody surfaces were covered with frost and the drag coefficient was high, the increase in drag coefficient as the angle of attack was increased was of the same order as the drag increase shown in figure 10 for similar conditions without afterbody frost formations.

At an angle of attack of 8°, a 53-percent rise in drag coefficient occurred within 3 minutes after the start of the icing condition. A peak value of drag coefficient, 0.0251, was obtained for this condition

after $30\frac{1}{2}$ minutes in the icing condition. Typical runback icing and afterbody frost formations at an 8° angle of attack are shown in figure 33. With a reduced water catch, the drag coefficient at a 5° angle of attack with practically no runback icing did not increase as rapidly as at 2° and 8° angles of attack. A peak value of 0.0143 (51-percent increase from initial bare airfoil drag), obtained after 41 minutes in the icing condition, was completely attributable to frost formations on the afterbody (fig. 34). Cessation of the water spray cloud in the tunnel results in gradual removal of the frost formation by wind forces, and to some extent by sublimation, with a consequent decrease in drag coefficient from the peak value.

2744

Leading-edge section cyclically de-iced. - With the leading-edge section intermittently heated as in cyclic operation of the de-icing equipment, frost formations on the afterbody again caused a rapid initial rise in drag coefficient (fig. 35). At a 5° angle of attack and a liquid-water content of 0.6 gram per cubic meter, the drag coefficient with a datum air temperature of 0° F increased from 0.0089 to 0.0123 (38 percent) in 2 minutes. This increase in drag coefficient was caused by frost formations on both airfoil surfaces and by leading-edge ice formations. At a datum air temperature of 25° F and a lower rate of water catch, the increase in drag coefficient at a 5° angle of attack was approximately 60 percent of that incurred at 0° F datum air temperature.

With a high rate of water catch and a datum air temperature of 0° F, the drag coefficient increased from 0.0089 to 0.0139 (56 percent) in 2 minutes, the latter value being attained after shedding of the leading-edge ice formation. The drag coefficient became somewhat stable at about 0.0158 as the time in icing was continued, and intermittent shedding of the leading-edge section had very little effect on the drag coefficient (fig. 36). For this particular run the upper surface remained unusually clear of frost. After a total time of 40 minutes in this icing condition, the angle of attack was changed from 5° to 8° during a heat-off period and the study was continued at the latter angle. In the first three cycles after the change in angle of attack to 8°, the ice on the lower surface was not completely shed. Photographs of the incomplete ice removal are shown in figure 37 together with a close-up of the frost formation on the afterbody. Although there was a marked reduction in drag coefficient at 8° angle of attack after each shedding cycle (fig. 35), the trend of drag coefficient was generally upward, reaching a peak value of 0.0218, which after ice shedding was reduced to 0.0194. It is apparent, therefore, that airfoil afterbody frost formations cause severe drag increases that cannot be appreciably reduced by use of current icing-protection systems.

In polar regions, sublimation frost accumulating on parked aircraft may be removed by various techniques before take-off; however, atmospheric conditions often occur whereby the aircraft again becomes coated with frost during the short period of taxiing and take-off. Such formations of frost have resulted in accidents in Alaska during World War II.

A brief study was made in the icing research tunnel of the effect of a sublimation frost on the drag of an airfoil. This study indicated that the drag may increase as much as 300 percent over the bare airfoil drag value. This increase in drag was obtained at an 8° angle of attack, an airspeed of 100 miles per hour, and a datum air temperature in the range of -25° to -8° F. A photograph of the frost formations causing this increase in drag is shown in figure 38. This drag increase must be considered conservative, because only the upper half-span of the airfoil model was covered with frost. Hence the momentum loss in the wake (measured at the center of the model span) did not measure the full drag change of the frost-covered section of the airfoil. The amount of frost shown in figure 38 was accumulated in about 5 minutes. The growth of the leading-edge frost formation was probably caused by a combination of frost and small condensation droplets, and close examination showed the microstructure of the formation to be very brittle and crystalline.

In addition to the large drag losses measured for a frost-covered airfoil, momentum wake considerations indicate that stalling characteristics of the airfoil have developed at low angles of attack, and the hazard of stalling at take-off is thereby introduced.

General comments on effect of frost on airfoil drag. - In general, frost formations over the entire airfoil (sublimation frost) or over the surfaces aft of the heatable areas cause a severe drag increase and at high angles of attack are accompanied by shifts in the position of the momentum wake which indicate a loss in lift and possible stall. Conventional heating systems (continuous or cyclic de-icing) do not remove a sufficient amount of frost to permit safe operation of the airfoil at high angles of attack where loss in lift is critical.

Correlation of Drag Caused by Icing with Drag Caused by Protuberances

The data presented herein are necessarily limited to specific operating and icing conditions; consequently, it is highly desirable to be able to extend the drag data associated with ice formations by comparative means. Reexamination of the aerodynamic effects of protuberances (fig. 39) at various positions on an airfoil (ref. 4) together with the effects of ice formations presented herein indicates that a large part

of the data in reference 4 is directly applicable for estimating the effect of ice formations on airfoil characteristics. From reference 4 it is apparent that protuberances near the stagnation region for low angles of attack do not greatly change the airfoil characteristics. A protuberance such as a mushroom-type ice formation (fig. 2(c)) is, of course, an exception. Reference 4 indicates that protuberances on the lower surface generally do not seriously affect the airfoil drag unless the protuberance is very large, as is also shown in the icing drag studies. Although the airfoil drag is affected in varying degrees by protuberances on the upper surface for all angles of attack, the most serious effects are obtained when the protuberances are near the leading edge, as was demonstrated by the serious drag increases caused by the leading-edge ice formations during the heat-off period of a cyclic de-icing system under conditions of high rates of water catch and high datum air temperature (figs. 21 to 24). The mushroom-type leading-edge ice formation and runback icing that forms in spanwise ridges can be represented by the spoiler protuberance of reference 4 (fig. 39(a)). A smoother, sheet-type runback ice formation can be represented by the faired protuberance (fig. 39(b)) used in reference 4. Such a faired protuberance generally does not affect the drag of an airfoil seriously except if located near the stagnation region on the upper surface of the airfoil. A protuberance located at a specific point on the lower surface will generally have a smaller percentage effect on drag as the angle of attack is increased.

2744

The data in reference 4 are directly applicable only to an NACA 0012 airfoil section and should not be applied to airfoils of thickness ratios greatly different from 12 percent. Because, however, the present airfoil model is of 12-percent thickness, the magnitude and trend of the aerodynamic changes caused by the protuberances of reference 4 are believed to be generally similar to those expected for an NACA 65_1-212 airfoil section. On the basis of this assumption, some of the data presented in reference 4 are replotted in figure 40 in terms of the percentage of drag increase as a function of protuberance height for the subject airfoil for three chord stations and three angles of attack. In addition to these data, limited data on a faired protuberance of 0.5-inch thickness (fig. 39(b)) indicate that a small increase of 0.0005 to 0.001 (6 to 10 percent of bare airfoil drag coefficient) may occur in the drag coefficient over the range of chord stations and angles of attack shown in figure 40. At the stagnation region, data for a spoiler protuberance faired on the downstream side (fig. 39(c)) indicated marked drag reduction as compared with an unfaired protuberance.

By discriminating use of the data of figure 40, reference 4, and the preceding discussion, the drag-coefficient change caused by ice formations can be estimated. However, the data presented herein and in reference 4 are limited in scope and all ice formations cannot be represented adequately by the simple protuberances investigated, especially those ice formations near the leading edge. In these cases only rough estimates of the effect of such ice formations can be made.

2744

For the runback ice formations shown in figures 11(c) and (d) near the 12-percent-chord station, the height of the ice formations on both the surfaces after 20 minutes of icing is estimated at between 1/8 and 3/16 inch. According to figure 40(c), this protuberance height should result in a drag increase of about 28 percent for each formation, or a total of 56 percent. On the upper surface, however, the ice formation is more nearly represented by a faired protuberance for which the drag increase amounts to about 6 percent (ref. 4). The total estimated drag increase would therefore be approximately 34 percent. The measured increase in drag for the ice formations in figure 11 was approximately 29 percent, which agrees satisfactorily with the estimated value.

In figures 21(c) and (e) the predominant ice formations are located at the leading edge of the upper surface and at about 13 percent of chord on the lower surface. Although there is an ice formation near 3 percent of chord on the lower surface, the effect of such a protuberance is overshadowed by the greater formation at 13 percent of chord. An estimate of the leading-edge ice from figures 21(c) and (e) indicates a thickness of about 1/2 inch, with the average thickness on the lower surface at 13 percent of chord about the same. By use of figures 40(a) and (c), the estimated drag-coefficient increase is about 101 percent compared with a measured increase in drag of 96 percent. For figure 21(d) much of the ice has been removed after the heating period, and the average ice thickness near the center span of the airfoil at 13 percent of chord is about 1/4 inch. Only thin faired runback streaks were evident on the upper surface, with a maximum thickness of about 0.1 inch which, according to reference 4 and substantiated by the drag measurements reported herein, can be neglected for drag evaluations. The total drag increase for this runback icing is estimated from figure 40(c) to be 46 percent compared with the measured increase in drag of 37 percent.

CH-3 back

The foregoing examples were selected to illustrate the degree to which the effect of ice formations on airfoil drag characteristics can be estimated. No such close agreement between estimated and measured increases in drag coefficient can be made for the dangerous ice formations occurring between 1 and 5 percent of chord on the airfoil upper surface without additional data similar to those presented in reference 4. The estimated drag values will usually tend to be high, because the ice formations are generally more faired and discontinuous than the protuberances used in reference 4.

Effect of Ice Formations on Lift and Moment Coefficients

The results of reference 4 show that protuberances on the lower surface do not greatly affect the slope of the lift curve or the maximum lift; in fact, these protuberances may even increase the lift slightly.

At low angles of attack, protuberances on the upper surface tend to decrease the lift slightly. At high angles of attack, however, protuberances on the upper surface have detrimental effects on the lift curve slope and the maximum lift coefficient, especially when the protuberance is located near the leading-edge radius region. According to reference 4, the effect of protuberances at a specific location on the airfoil upper surface is generally to decrease the maximum lift coefficient nearly proportionally to the protuberance height; however, protuberances near the leading edge cause disproportionately large decreases in lift. Although the change in lift coefficient due to ice formations could not be established, the shift in the momentum wake behind the airfoil (discussed previously) provided a good indication of a large change in lift and an approach to an airfoil stall condition. Such indications of stall were usually caused by large mushroom-type ice formations, heavy runback icing, or frost on the airfoil upper surface at the leading-edge radius region. In the absence of more exact corroborative data, it would appear that changes in lift due to ice formations can be estimated from reference 4.

In general, the effect of protuberances and hence ice formations on the moment coefficient appears to be negligible except for large ice protuberances on the upper surface forward of the maximum thickness location of the airfoil. Large protuberances, especially near the leading edge, cause a more negative slope and a sharp break in the moment-coefficient curve (ref. 4).

Significance of Results

In the interpretation of the significance of the data presented in the preceding sections, consideration must be taken of the probability, frequency, and duration of encountering icing conditions that would cause serious increases in drag and losses in lift during flight. For example, the data for a condition of high rate of water catch and high datum air temperature indicate large drag increases at high angles of attack; however, such an attitude is generally of short duration for the aircraft and occurs primarily during the initial take-off or the final let-down stages. On the other hand, a condition of high rate of water catch and high datum air temperature at a low angle of attack may occur relatively frequently for jet-powered fighter or bomber aircraft; consequently, this icing and operating condition may be of much greater interest with respect to drag changes and aircraft performance.

With the possibility of frost formations on airfoil afterbodies in flight assumed negligible, it would appear that low rates of water catch - generally obtained by a combination of small droplets, average liquid-water content, low subsonic airspeeds, and large airfoil chords and thicknesses - do not seriously affect the airfoil drag characteristics. For these same conditions of low water catch, cyclic de-icing of the leading-edge section does not improve the drag characteristics of the airfoil, principally because the airfoil drag is not seriously affected

2744

by the primary leading-edge ice formations (fig. 15). The formation of runback ice aft of the heated areas, caused by either a cyclic de-icing system or a continuously heated system which does not evaporate all the impinging water, therefore constitutes the major means of incurring a drag penalty. These drag penalties are, however, of small magnitude over the normal range of icing conditions generally encountered by jet aircraft in flight, and the loss in lift associated with these drag penalties is negligible (refs. 4 and 5). It appears, therefore, that for large airfoil chords and for thicknesses of the same magnitude as the airfoil studied, no icing protection is required for a condition of low rate of water catch and streamlined ice formation.

2744

It should be noted that these comments apply specifically to the 12-percent-thick airfoil section investigated. Use of smaller chord or thinner airfoils will result in higher and more rapid drag-coefficient increases and possibly a more serious deterioration in lift for comparable ice formations. The initial drag coefficient of the bare airfoil was in the range generally associated with standard roughness, for which some surface waviness, dustiness, and protective coating may be present. It is believed that if a completely clean and aerodynamically smooth airfoil were exposed to icing conditions, the drag coefficient would quickly rise, especially in the low-drag range, by as much as 100 percent to approach the initial drag coefficients reported herein for the bare airfoil. Thereafter ice formations of the streamlined type would contribute no appreciable drag increase.

A mushroom-type glaze-ice formation resulting from icing encounters with combinations of high liquid-water content, large droplet size, high airspeed, and high datum air temperatures will cause large and rapid increases in drag for which most aircraft may require protection. From the data presented in figures 20 and 25 it is apparent that an airfoil equipped with a cyclic de-icing system is most susceptible to drag penalties at high angles of attack and during approach operation. It is therefore essential that high angles of attack be avoided if a heavy deposit of mushroom-type glaze ice has been incurred on the leading edge. Proper operation of the aircraft, by shedding of heavy leading-edge ice formations before assuming an approach attitude, should minimize the danger of stalling the airfoil.

Runback ice formations on the lower surface increase the drag somewhat but do not appear to affect seriously the airfoil aerodynamic characteristics. If the upper surface of an airfoil is subject to little or no runback icing and the lower surface is permitted to accumulate runback icing, a substantial reduction in heating requirements over those calculated in reference 1 can be achieved. Thus, the use of a continuous heating system might be extended to protect high-altitude, high-speed, turbojet-powered aircraft without the large performance penalties indicated in reference 1 for a system designed to evaporate all the impinging water.

For certain types of aircraft that need only penetrate a stratus cloud layer immediately after take-off and are capable of rapid descent through such a cloud layer, the magnitude of the ice formation accumulated during the flight through the layer may not seriously affect the aircraft performance. Upon ascent, the ice formations may decrease by sublimation at high altitude and high speed at rates up to 1 inch of thickness per hour. Should the expected accumulation of ice formations on an airfoil during descent prove incompatible with the aircraft performance specifications, an icing-protection system may be included that is designed to operate only for low-speed let-down conditions. Such an icing-protection system could operate either cyclically or continuously with a relatively low heating requirement.

2744

The icing of an aircraft in flying through a cumulus cloud at high altitude should not prove excessively detrimental to aircraft performance, because the aircraft will in all probability be at a low angle of attack, a flight condition not conducive to large changes in airfoil performance characteristics.

Although the possibility exists of forming frost on aircraft surfaces during flight, the probability of such an occurrence appears to be quite remote. Frost formations during ground operation, however, are quite common in cold climates and, with respect to the drag losses associated with such formations on airfoil surfaces, merit attention. The use of a conventional thermal icing-protection system to remove frost from the leading-edge region of an airfoil will not provide sufficient protection to ensure a safe take-off. It is, therefore, necessary in all-weather operation to provide additional protection from frost for the aircraft while on the ground, such as sheltering the wings and empennage surfaces with heated covers, tents, or hangars.

SUMMARY OF RESULTS

The results of an investigation of the effects of ice and frost formations on the drag of an NACA 65_1-212 airfoil section may be summarized as follows:

1. At high angles of attack (8°), a prohibitive increase in drag coefficient of approximately 70 percent was obtained within 2 minutes when ice formed on the upper surface near the leading edge of the airfoil under conditions of heavy glaze icing (high rate of water catch and high datum air temperatures).

2. Relatively small formations of glaze icing (low rates of water catch and high datum air temperature) increased the drag coefficient of the airfoil over the range of conditions studied by less than 27 percent following a 30-minute icing period, except for simulated landing

approaches. Rime-ice formations associated with lower air temperatures did not increase the airfoil drag coefficient appreciably above the initial (standard roughness) level, even with high rates of water catch.

3. A glaze-ice formation on the leading-edge section for a simulated approach condition, during which the airfoil attitude is increased from 2° to 8° angle of attack, caused a severe increase in drag coefficient of over 285 percent over the bare airfoil drag at 8° angle of attack and was accompanied by a shift in the position of the momentum wake that indicated incipient stalling of the airfoil.

2744

4. Runback icing on the lower surface obtained with the use of a continuous heating system that does not evaporate all the impinging water caused moderate drag increases only when a spanwise ridge of ice was formed aft of the heatable area.

5. Removal of the primary ice formations by cyclic de-icing caused the drag to return almost to the bare airfoil drag coefficient, except for the drag caused by runback ice formations. In general, runback icing with a cyclic de-icing system increased the drag less than did runback icing incurred in similar conditions with a continuous heating system that only evaporated approximately 28 to 44 percent of the impinging water.

6. Frost formations on the airfoil surfaces caused a large and rapid increase in the drag coefficient and at high angles of attack (8°) were accompanied by incipient stalling of the airfoil.

Lewis Flight Propulsion Laboratory
National Advisory Committee for Aeronautics
Cleveland, Ohio

REFERENCES

1. Gelder, Thomas F., Lewis, James P., and Koutz, Stanley L.: Icing Protection for Turbojet Transport Airplane: Heating Requirements, Methods of Protection, and Performance Penalties. NACA TN 2866, 1953.

2. Gray, V. H., Bowden, D. T., and von Glahn, U.: Preliminary Results of Cyclical De-Icing of a Gas-Heated Airfoil. NACA RM E51J29, 1952.

3. Lewis, James P., and Bowden, Dean T.: Preliminary Investigation of Cyclic De-Icing of an Airfoil Using an External Electric Heater. NACA RM E51J30, 1952.

4. Jacobs, Eastman N.: Airfoil Section Characteristics as Affected by Protuberances. NACA Rep. 446, 1932.

5. Gulick, Beverly G. : Effect of a Simulated Ice Formation on the Aerodynamic Characteristics of an Airfoil. NACA WR L 292, 1938.

6. Perkins, Porter J., McCullough, Stuart, and Lewis, Ralph D.: A Simplified Instrument for Recording and Indicating Frequency and Intensity of Icing Conditions Encountered in Flight. NACA RM E51E16, 1951.

7. Gray, Vernon H., and Bowden, Dean T.: Comparison of Several Methods of Cyclic De-Icing of a Gas-Heated Airfoil. NACA RM E53C27, 1953.

2744

2744

CH-4

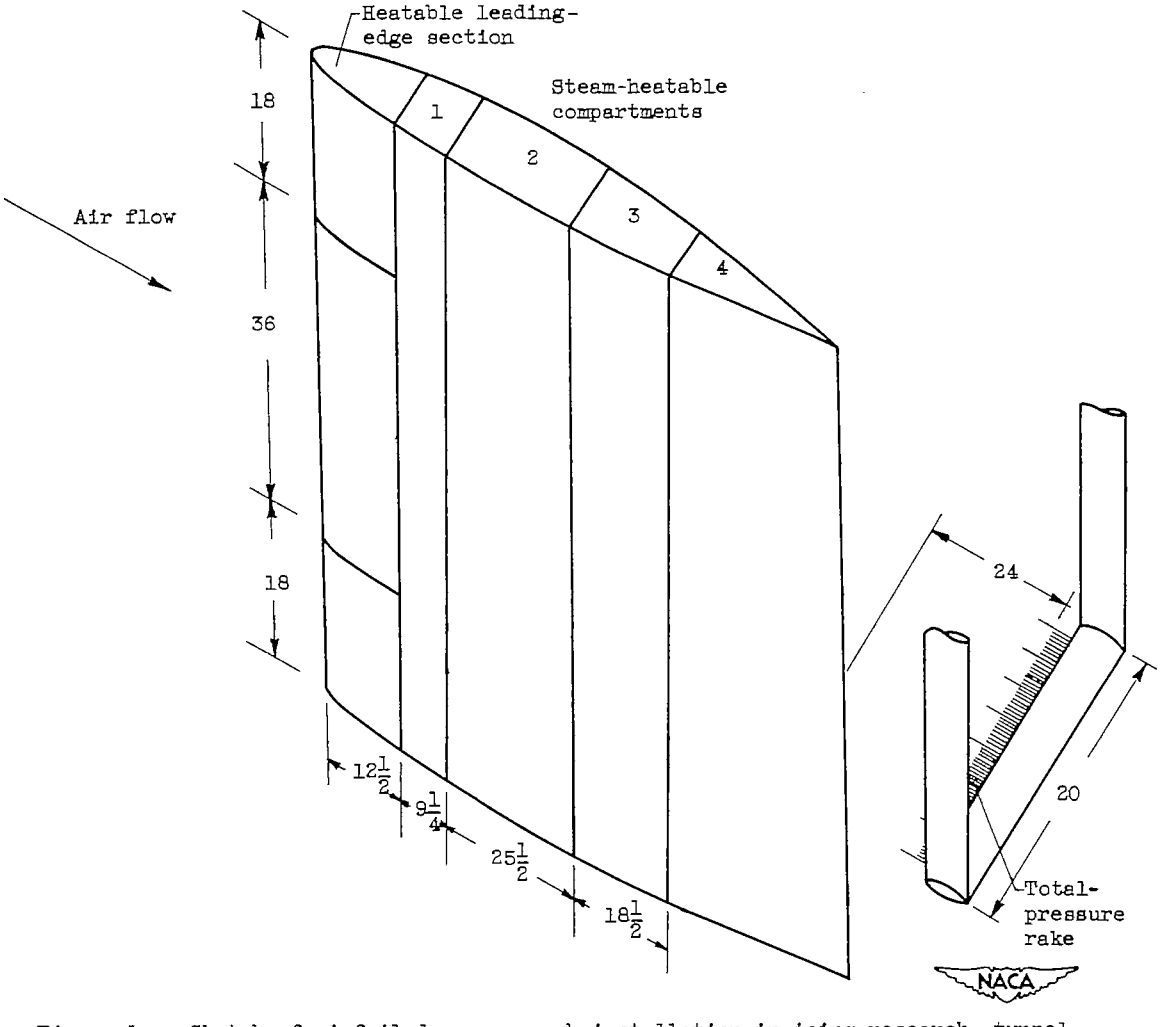

Figure 1. - Sketch of airfoil drag research installation in icing research tunnel. (Dimensions are in inches.)

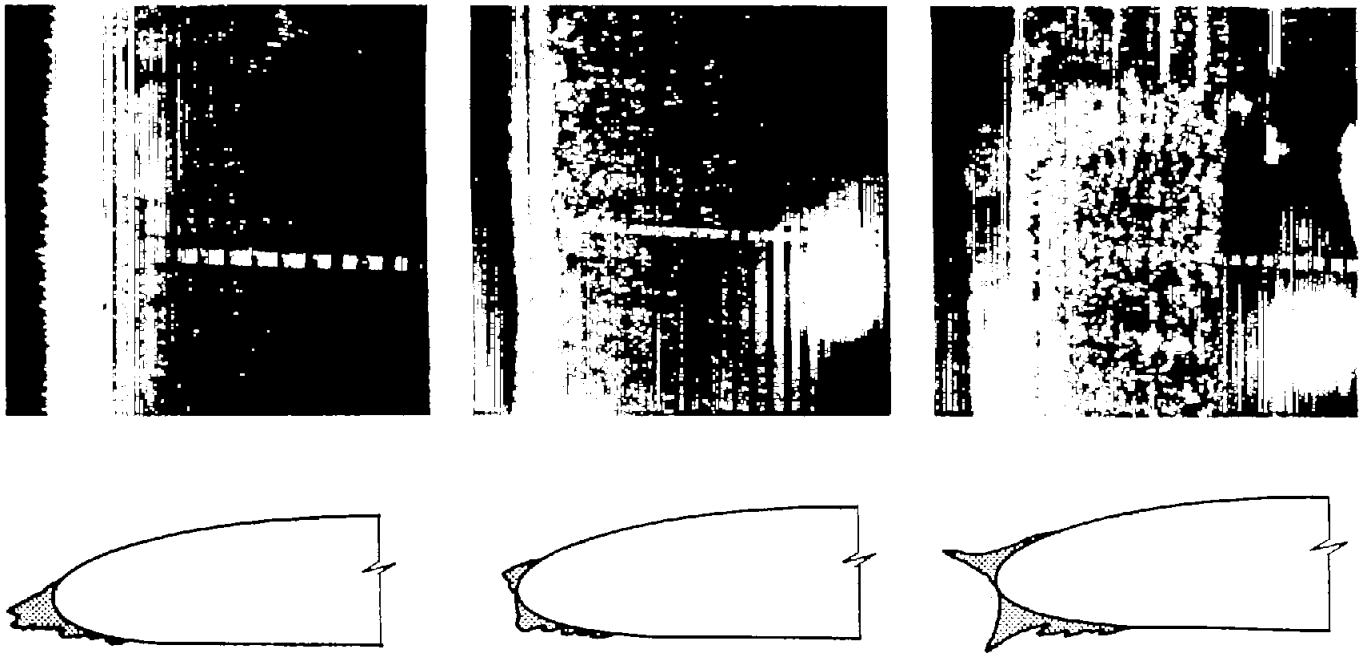

(a) Rime ice. Datum air temperature, 0° F.

(b) Glaze ice. Datum air temperature, 25° F; low rate of water catch.

(c) Double-peak mushroom-type glaze ice. Datum air temperature, 25° to 30° F; moderate to high rate of water catch.

NACA

C-31278

Figure 2. - General types of primary icing observed on airfoil leading edge.

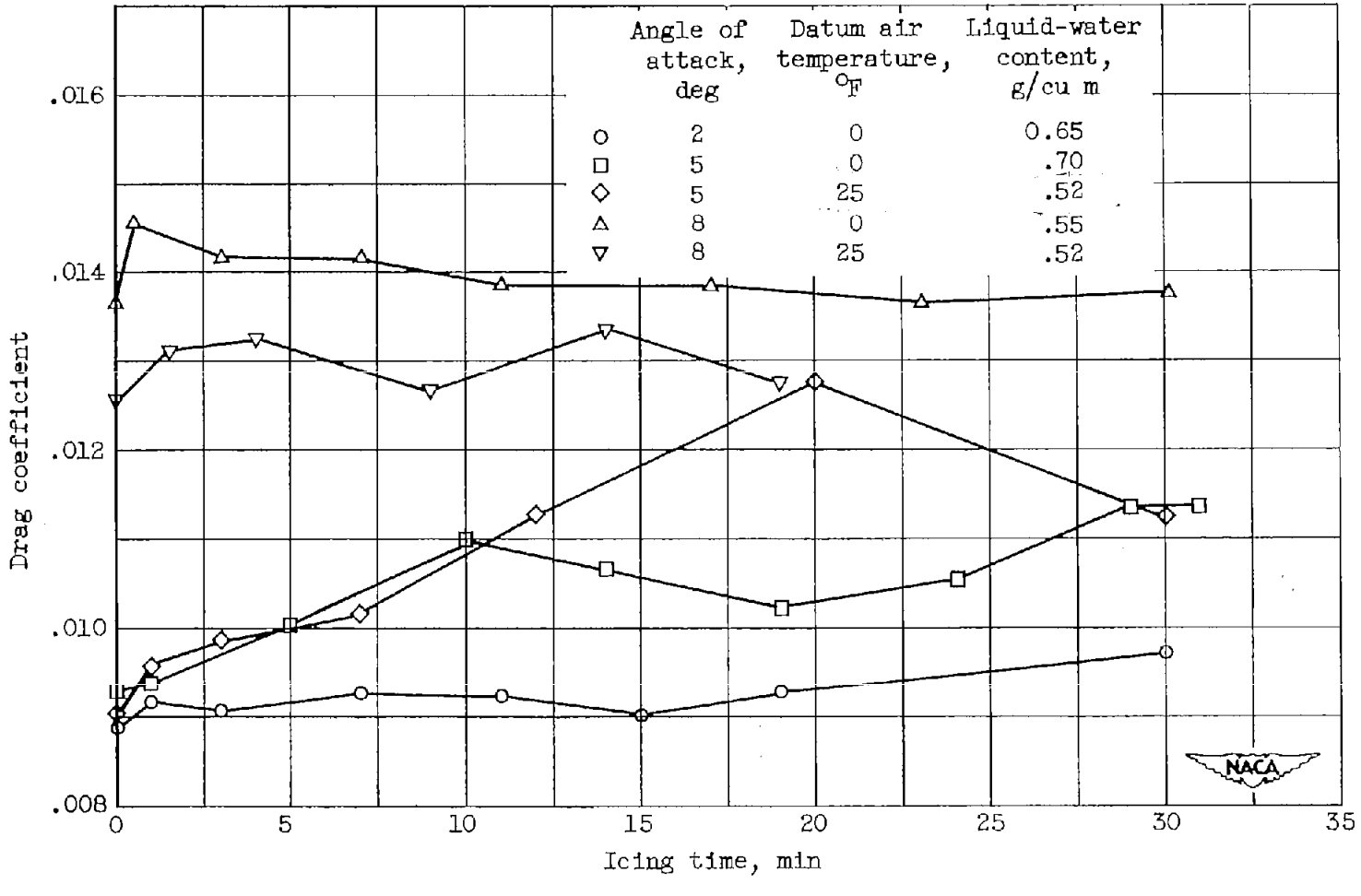

Figure 3. - Drag coefficient as function of time in icing with leading-edge section unheated and no afterbody frost formations. Airspeed, 260 miles per hour.

2744

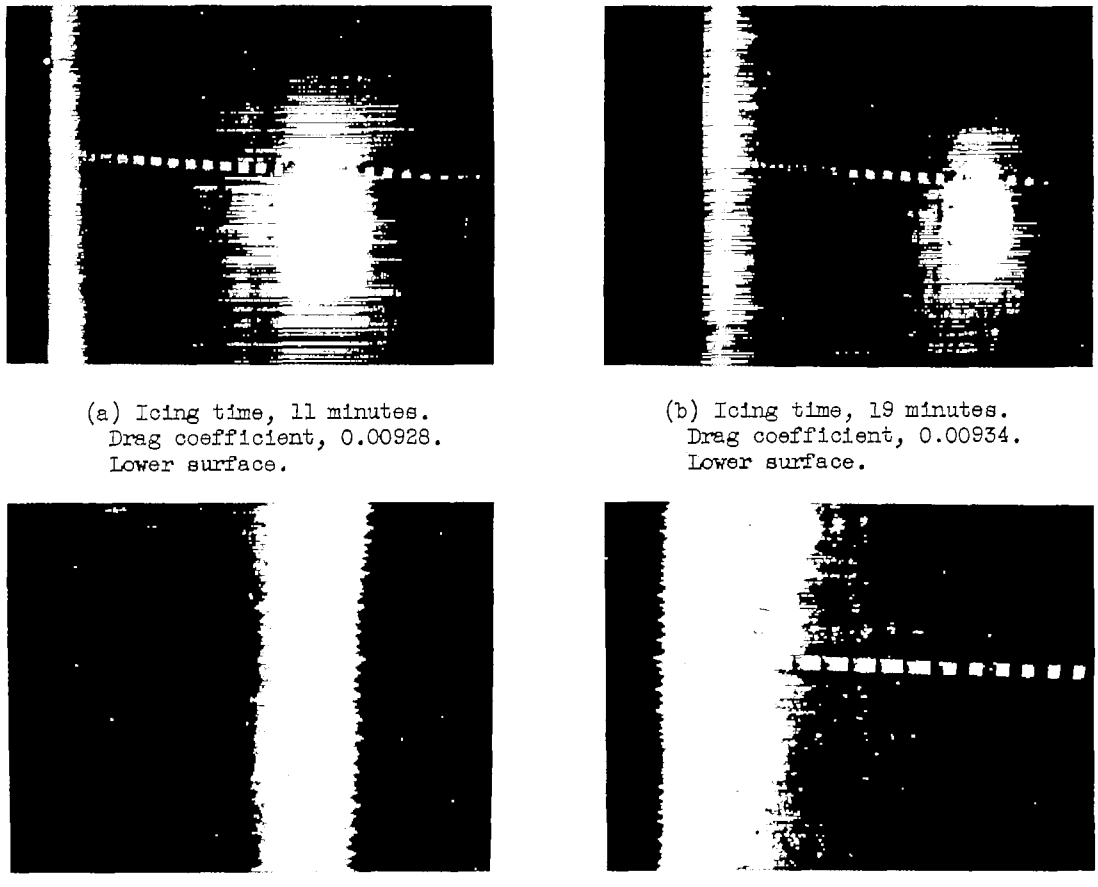

(a) Icing time, 11 minutes.
Drag coefficient, 0.00928.
Lower surface.

(b) Icing time, 19 minutes.
Drag coefficient, 0.00934.
Lower surface.

(c) Icing time, 31 minutes.
Drag coefficient, 0.00964.
Upper surface.

C-31279

(d) Icing time, 31 minutes.
Drag coefficient, 0.00964.
Lower surface.

Figure 4. - Typical rime-ice formations on unheated airfoil leading-edge section at 2° angle of attack. Airspeed, 260 miles per hour; datum air temperature, 0° F; liquid-water content, 0.65 gram per cubic meter; initial drag coefficient, 0.0089.

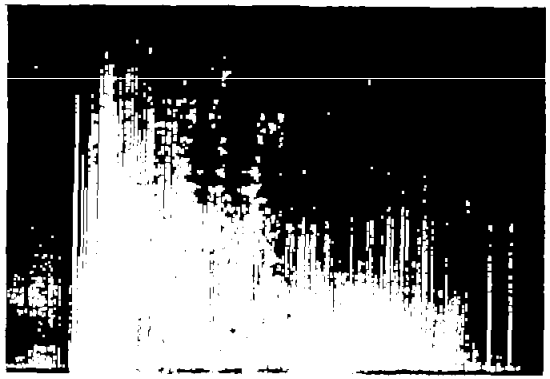

(a) Icing time, 10 minutes. Drag coefficient, 0.0110. Lower surface.

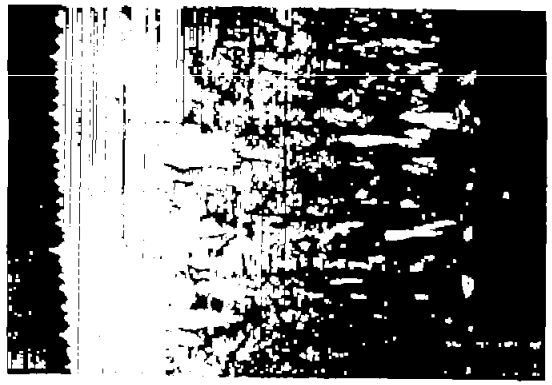

(b) Icing time, $27\frac{1}{2}$ minutes. Drag coefficient, 0.0109. Lower surface.

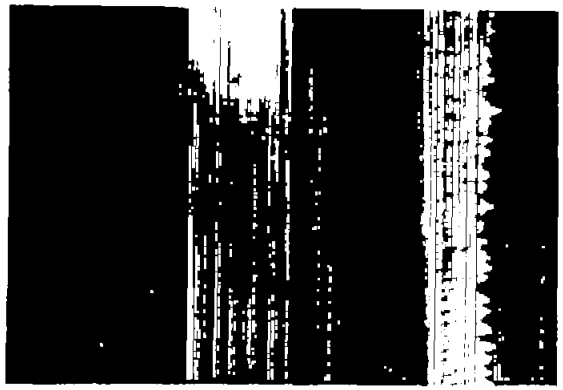

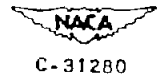

C-31280

(c) Icing time, $27\frac{1}{2}$ minutes. Drag coefficient, 0.0100. Upper surface.

Figure 5. - Typical rime-ice formations on unheated airfoil leading-edge section at 5° angle of attack. Airspeed, 260 miles per hour; datum air temperature, 0° F; liquid-water content, 0.70 gram per cubic meter; initial drag coefficient, 0.0109.

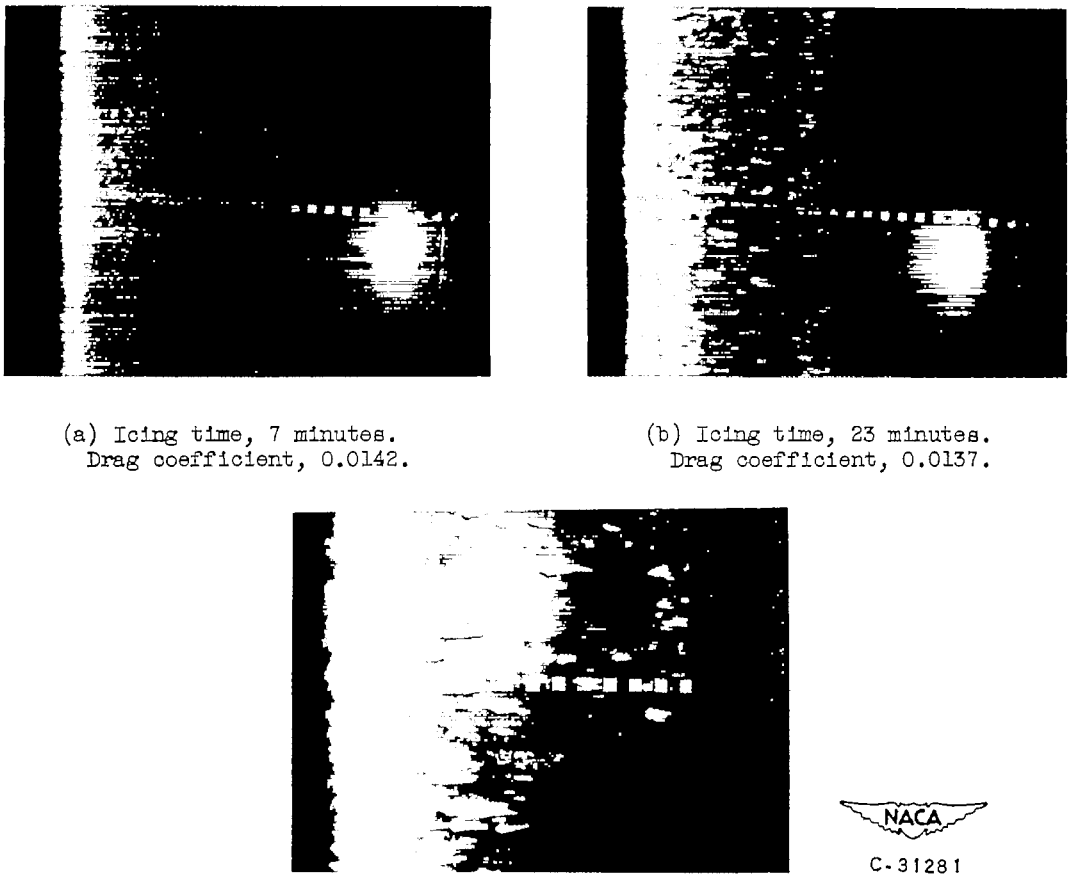

(a) Icing time, 7 minutes.
Drag coefficient, 0.0142.

(b) Icing time, 23 minutes.
Drag coefficient, 0.0137.

(c) Icing time, $31\frac{1}{2}$ minutes.
Drag coefficient, 0.0138.

Figure 6. - Typical rime-ice formations on lower surface of unheated airfoil leading-edge section at 8° angle of attack. Airspeed, 260 miles per hour; datum air temperature, 0° F; liquid-water content, 0.55 gram per cubic meter; initial drag coefficient, 0.0137.

2744

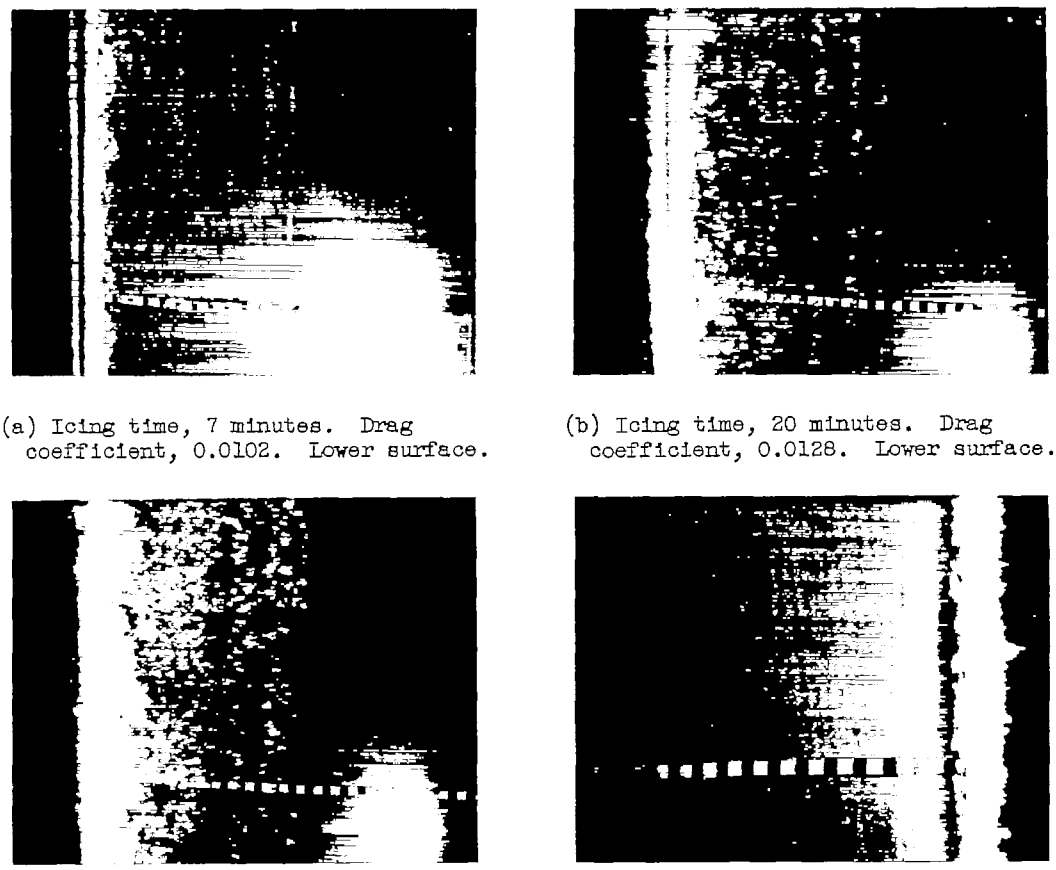

(a) Icing time, 7 minutes. Drag coefficient, 0.0102. Lower surface.

(b) Icing time, 20 minutes. Drag coefficient, 0.0128. Lower surface.

(c) Icing time, 30 minutes. Drag coefficient, 0.0113. Lower surface.

C-31283

(d) Icing time, 30 minutes. Drag coefficient, 0.0113. Upper surface.

Figure 7. - Typical glaze-ice formations with low rate of water catch on unheated airfoil leading-edge section at 5° angle of attack. Airspeed, 260 miles per hour; datum air temperature, 25° F; liquid-water content, 0.52 gram per cubic meter; initial drag coefficient, 0.00904.

2744

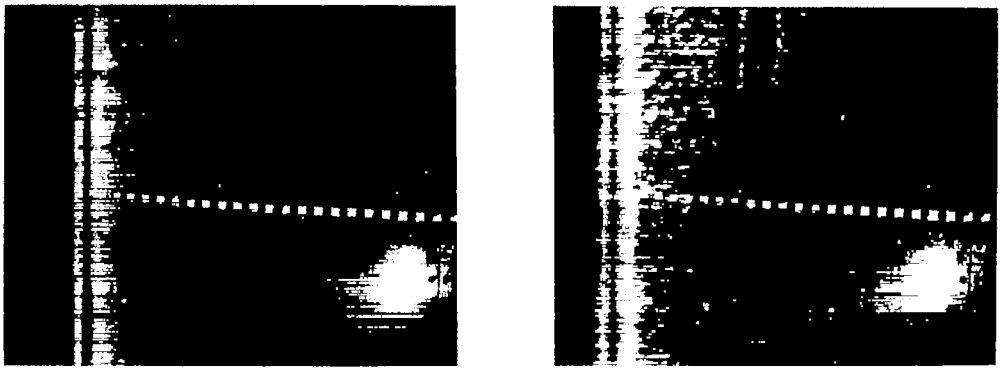

(a) Icing time, 4 minutes.
Drag coefficient, 0.0133.

(b) Icing time, 14 minutes.
Drag coefficient, 0.0134.

Figure 8. - Typical glaze-ice formations with low rate of water catch on lower surface of unheated airfoil leading-edge section at 8° angle of attack. Airspeed, 260 miles per hour; datum air temperature, 25° F; liquid-water content, 0.52 gram per cubic meter; initial drag coefficient, 0.0126.

C-31284

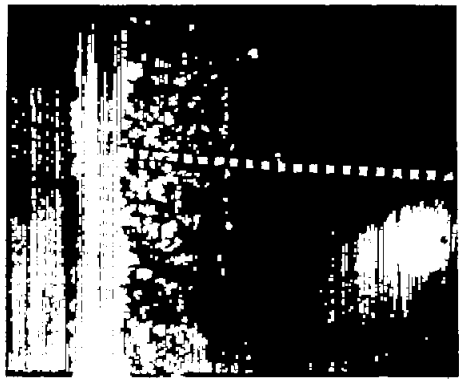

(a) Airspeed, 260 miles per hour; datum air temperature, 30° F; liquid-water content, 0.52 gram per cubic meter; angle of attack, 8°; icing time, 28 minutes; initial drag coefficient, 0.0128; drag coefficient with ice, 0.0222.

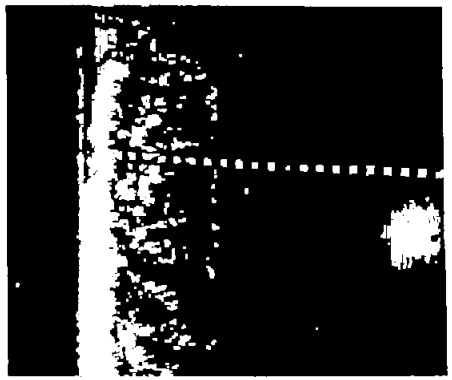

(b) Airspeed, 260 miles per hour; datum air temperature, 30° F; liquid-water content, 0.52 gram per cubic meter; angle of attack, 8°; icing time, 33 minutes; initial drag coefficient, 0.0128; drag coefficient with ice, 0.0153.

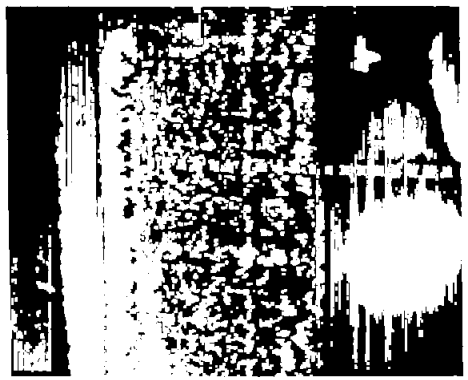

(c) Airspeed, 180 miles per hour; datum air temperature, 29° F; liquid-water content, 1.4 grams per cubic meter; angle of attack, 5°; icing time, 24 minutes; initial drag coefficient, 0.00958; drag coefficient with ice, 0.0241.

C-31285

Figure 9. - Typical heavy mushroom-type glaze-ice formations on lower surface of unheated airfoil leading-edge section.

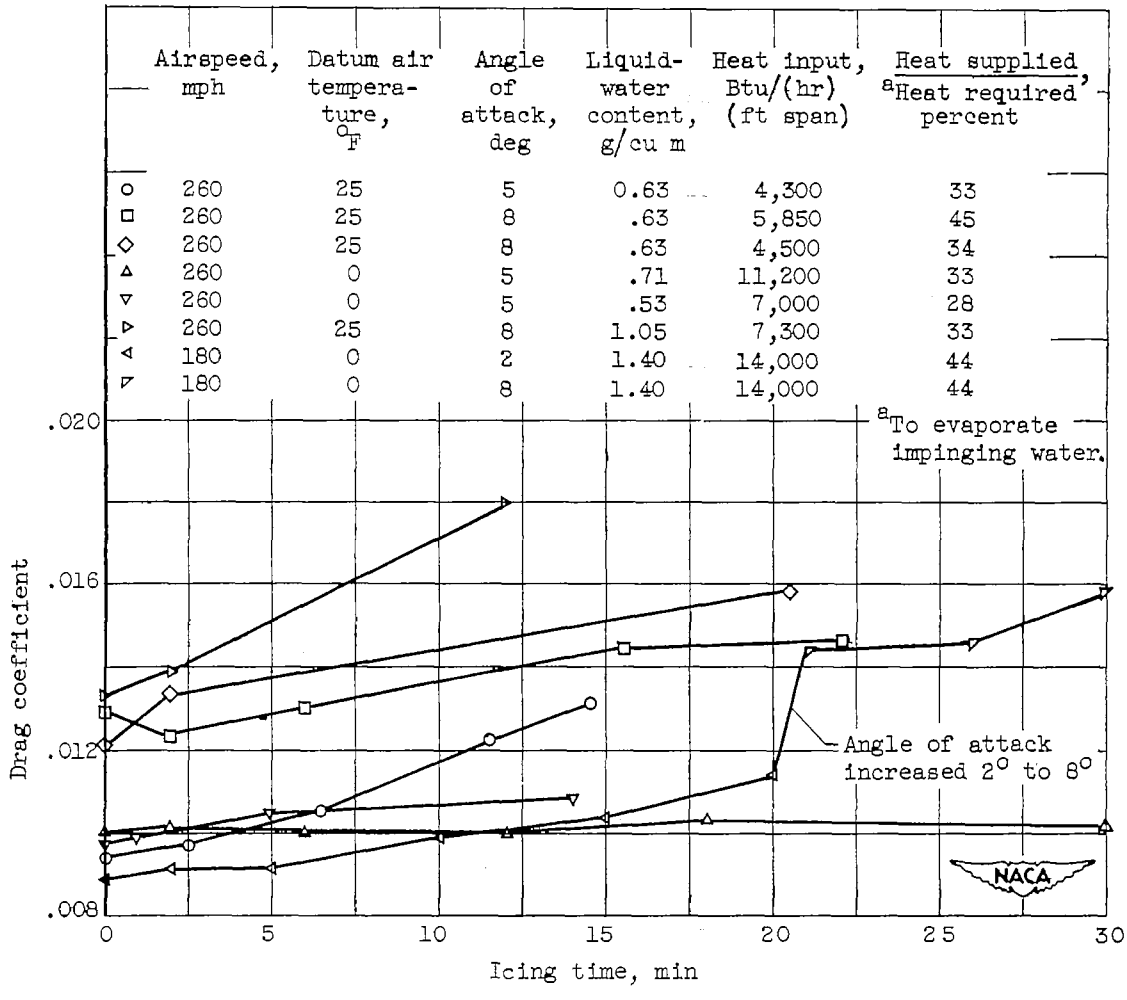

Figure 10. - Effect of runback icing on drag coefficient as function of time in icing with leading-edge section continuously heated and no afterbody frost formations.

2744
CH-5 back

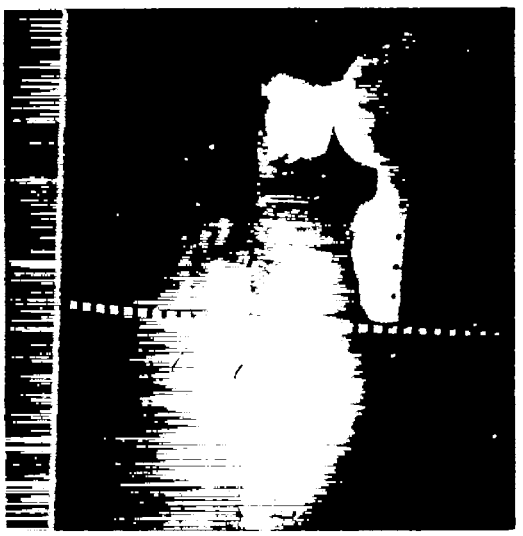

(a) Icing time, 5 minutes. Drag coefficient, 0.00909. Lower surface.

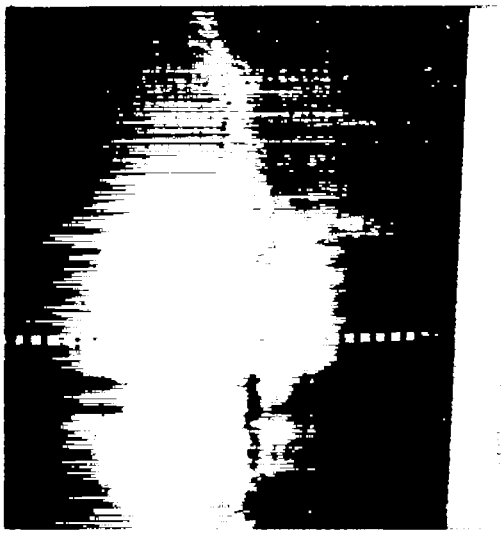

(b) Icing time, 10 minutes. Drag coefficient, 0.0098. Upper surface.

(c) Icing time, 15 minutes. Drag coefficient, 0.0103. Lower surface.

(d) Icing time, 20 minutes. Drag coefficient, 0.0113. Upper surface.

C-31286

Figure 11. - Typical runback icing with high rate of water catch on airfoil at 2° angle of attack with leading-edge section continuously heated. Airspeed, 180 miles per hour; datum air temperature, 0° F; liquid-water content, approximately 1.4 grams per cubic meter; initial drag coefficient, 0.0088.

2744

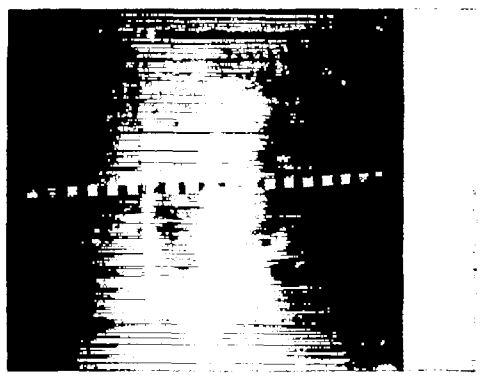

(a) Icing time, $6\frac{1}{2}$ minutes.
Drag coefficient, 0.0105.
Upper surface.

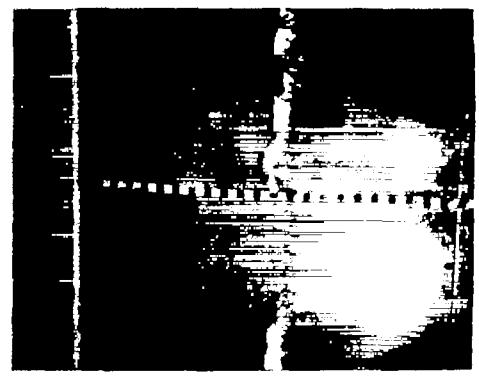

(b) Icing time, $11\frac{1}{2}$ minutes.
Drag coefficient, 0.0122.
Lower surface.

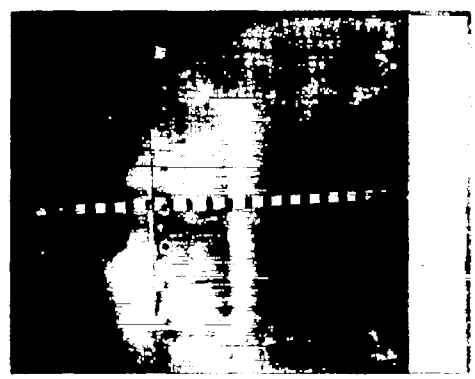

C-31287

(c) Icing time, $14\frac{1}{2}$ minutes.
Drag coefficient, 0.0131.
Upper surface.

Figure 12. - Typical runback icing with low rate of water catch on airfoil at 5° angle of attack with leading-edge section continuously heated. Airspeed, 260 miles per hour; datum air temperature, 25° F; liquid-water content, 0.63 gram per cubic meter; initial drag coefficient, 0.00943.

2744

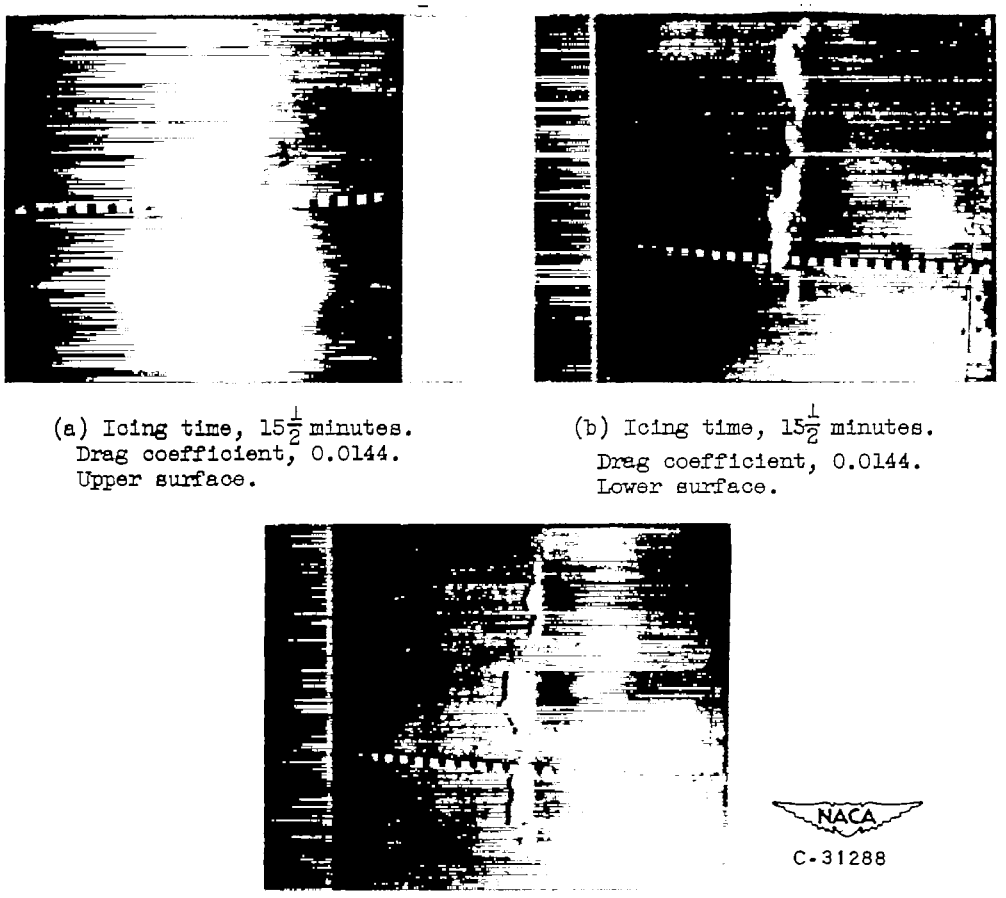

(a) Icing time, $15\frac{1}{2}$ minutes. Drag coefficient, 0.0144. Upper surface.

(b) Icing time, $15\frac{1}{2}$ minutes. Drag coefficient, 0.0144. Lower surface.

(c) Icing time, 22 minutes. Drag coefficient, 0.0146. Lower surface.

Figure 13. - Typical runback icing with low rate of water catch on airfoil at 8° angle of attack with leading-edge section continuously heated. Airspeed, 260 miles per hour; datum air temperature, 25° F; liquid-water content, 0.63 gram per cubic meter; initial drag coefficient, 0.0129.

2744

(a) Icing time, 29 minutes. Drag coefficient, 0.0217. Upper surface.

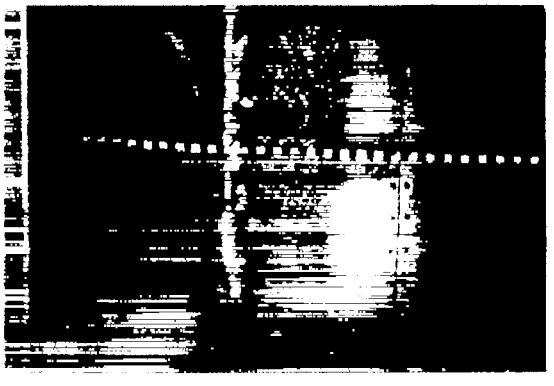

(b) Icing time, 29½ minutes. Drag coefficient, 0.0217. Lower surface.

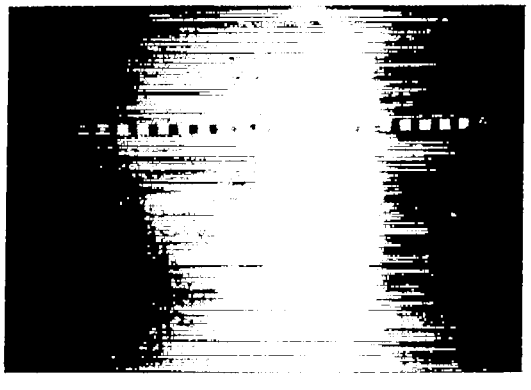

NACA

C-31289

(c) Icing time, 40 minutes. Drag coefficient, 0.0175. Upper surface.

Figure 14. - Typical runback icing with high rate of water catch on airfoil at 8° angle of attack with leading-edge section continuously heated. Airspeed, 260 miles per hour; datum air temperature, 25° F; liquid-water content, 1.05 grams per cubic meter; initial drag coefficient, 0.0129.

2744

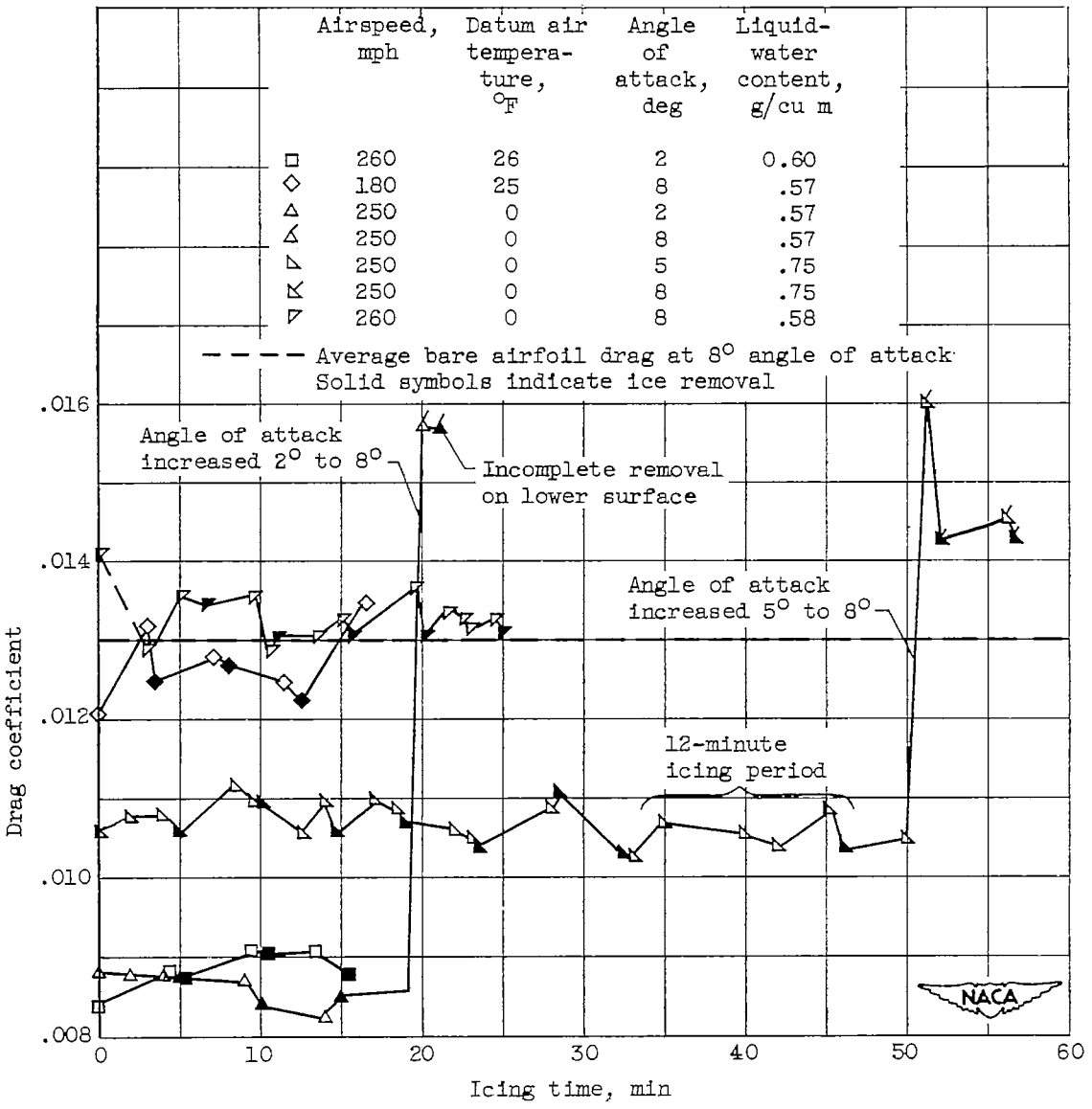

Figure 15. - Effect of streamlined ice formations on drag coefficient as function of time in icing with leading-edge section cyclically de-iced and no afterbody frost formations.

2744

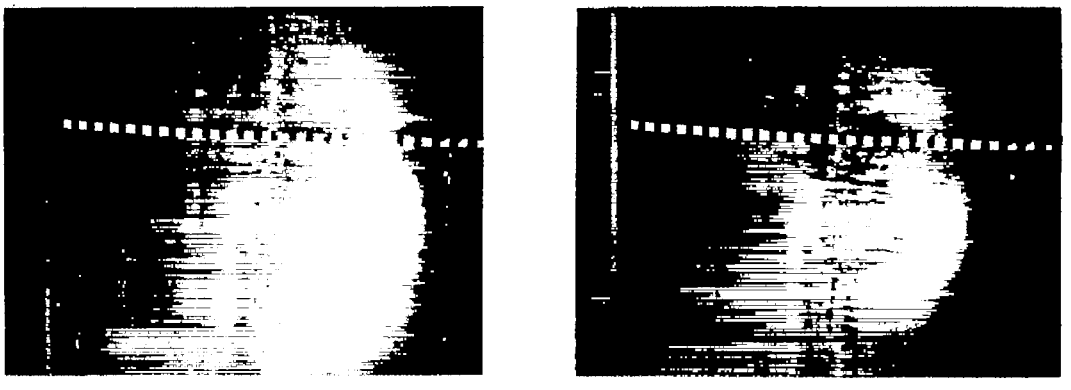

(a) Icing time, $13\frac{1}{2}$ minutes.
Drag coefficient, 0.0091.
Before ice removal.

(b) Icing time, $15\frac{1}{2}$ minutes.
Drag coefficient, 0.0088.
After ice removal.

Figure 16. - Typical glaze-ice formations with low rate of water catch on lower surface of cyclically de-iced airfoil leading-edge section at 2° angle of attack. Airspeed, 260 miles per hour; datum air temperature, 26° F; liquid-water content, 0.60 gram per cubic meter; initial drag coefficient, 0.00836; icing period, approximately 260 seconds; heat-on period, 15 seconds.

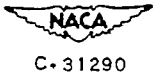

C-31290

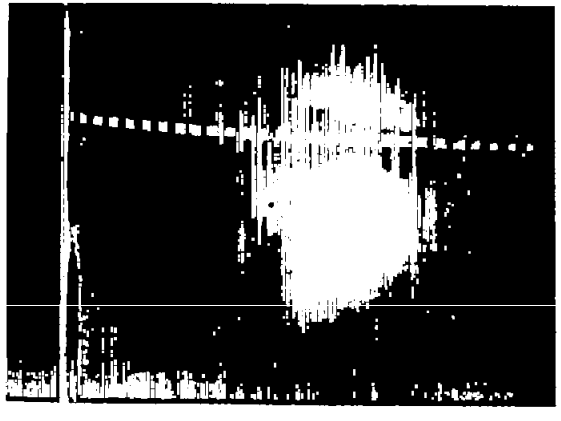

(a) Icing time, 9 minutes. Drag coefficient, 0.00877. Lower surface, before ice removal.

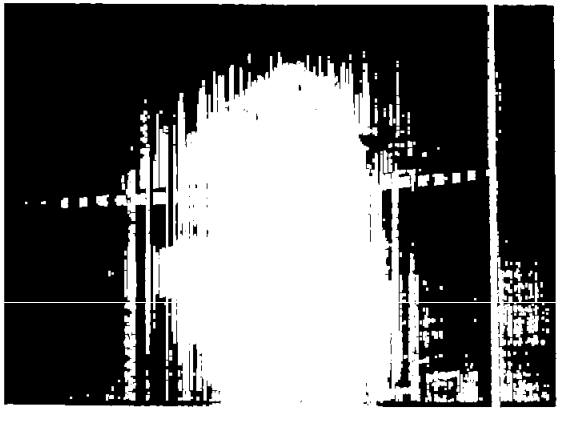

(b) Icing time, 14 minutes. Drag coefficient, 0.00822. Upper surface, before ice removal.

Figure 17. - Typical rime and runback icing formations with low rate of water catch on airfoil with cyclically de-iced leading-edge section at 2° angle of attack. Airspeed, 250 miles per hour; datum air temperature, 0° F; liquid-water content, 0.57 gram per cubic meter; initial drag coefficient, 0.00665; icing period, approximately 260 seconds; heat-on period, 17 seconds.

C-31282

2744

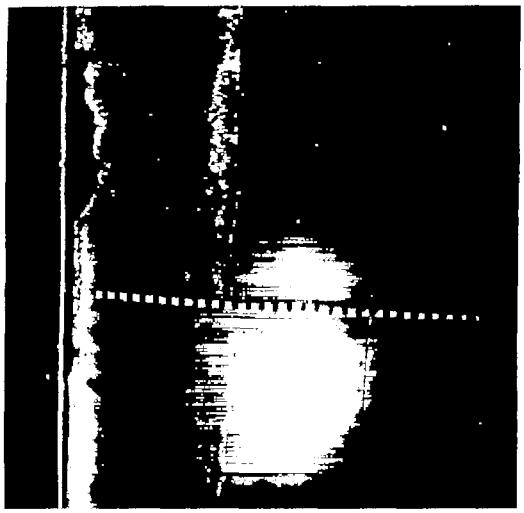

(a) Icing time, 14 minutes. Drag coefficient, 0.0110. Before ice removal. Icing period, approximately 260 seconds.

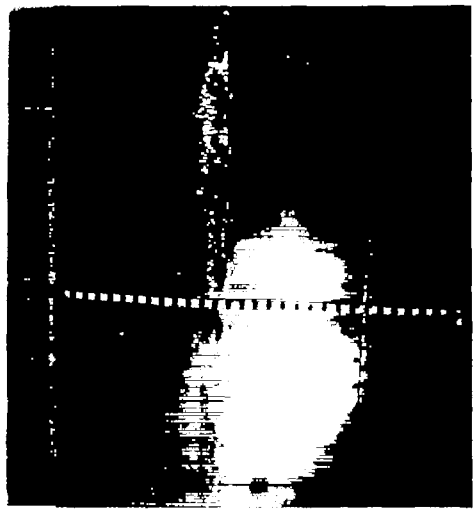

(b) Icing time, $14\frac{1}{2}$ minutes. Drag coefficient, 0.0106. After ice removal.

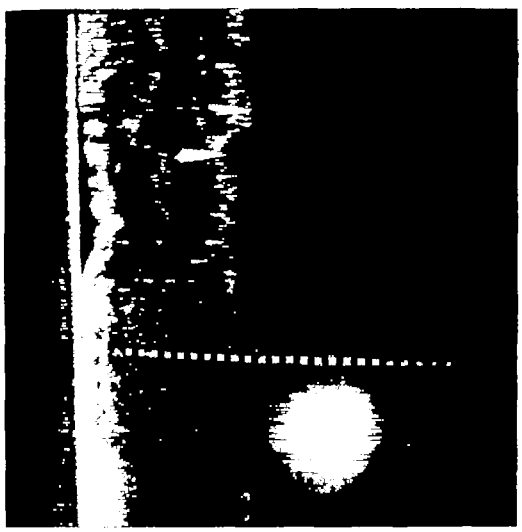

(c) Icing time, 45 minutes. Drag coefficient, 0.0109. Before ice removal. Icing period, approximately 720 seconds.

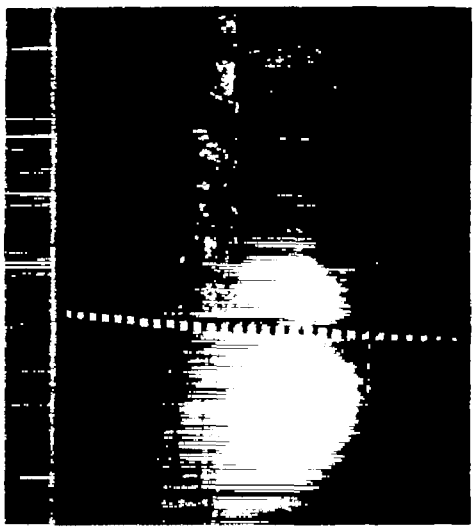

(d) Icing time, 46 minutes. Drag coefficient, 0.0104. After ice removal.

C-31291

Figure 18. - Typical rime and runback icing formations with low rate of water catch on lower surface of airfoil with cyclically de-iced leading-edge section at 5° angle of attack. Airspeed, 250 miles per hour; datum air temperature, 0° F; liquid-water content, 0.75 gram per cubic meter; initial drag coefficient, 0.0106; heat-on period, 17 seconds.

2744

CH-6 back

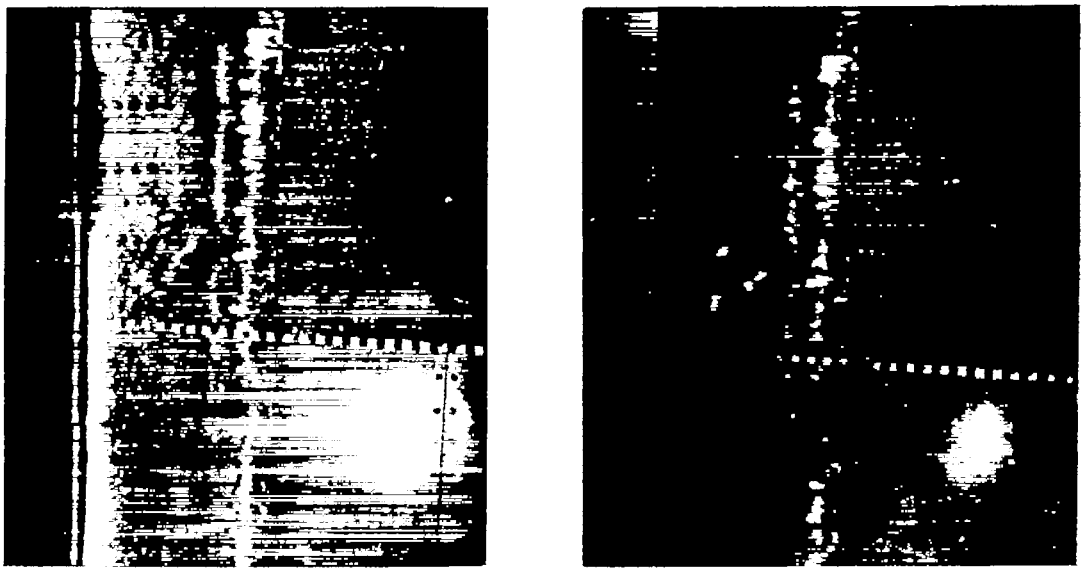

(a) Icing time, 15 minutes.
Drag coefficient, 0.0133.
Before ice removal.

(b) Icing time, $15\frac{1}{2}$ minutes.
Drag coefficient, 0.0131.
After ice removal.

C-31292

Figure 19. - Typical rime and runback icing formations with low rate of water catch on lower surface of airfoil with cyclically de-iced leading-edge section at 8° angle of attack. Airspeed, 260 miles per hour; datum air temperature, 0° F; liquid-water content, 0.58 gram per cubic meter; initial drag coefficient, 0.0141; icing period, approximately 260 seconds; heat-on period, 17 seconds.

2744

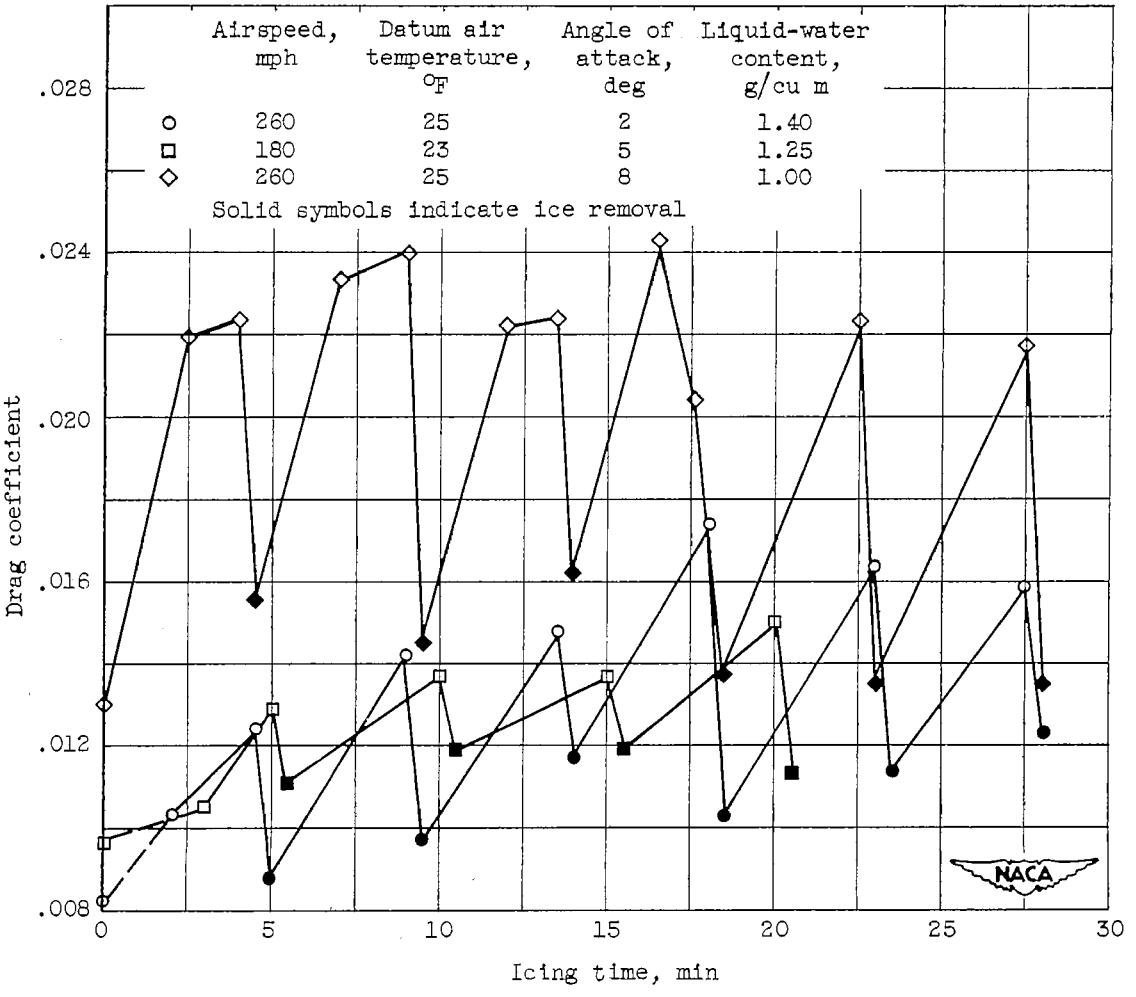

Figure 20. - Effect of mushroom-type glaze-ice formations on drag coefficient as function of time in icing with leading edge cyclically de-iced and no afterbody frost formations.

2744

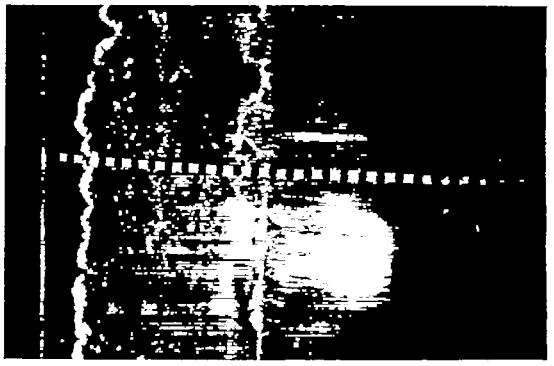

(a) Icing time, $8\frac{1}{2}$ minutes.
Drag coefficient, 0.0142.
Lower surface, before ice removal.

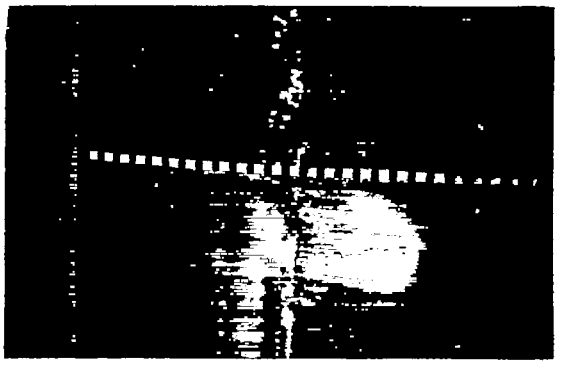

(b) Icing time, $9\frac{1}{2}$ minutes.
Drag coefficient, 0.00973.
Lower surface, after ice removal.

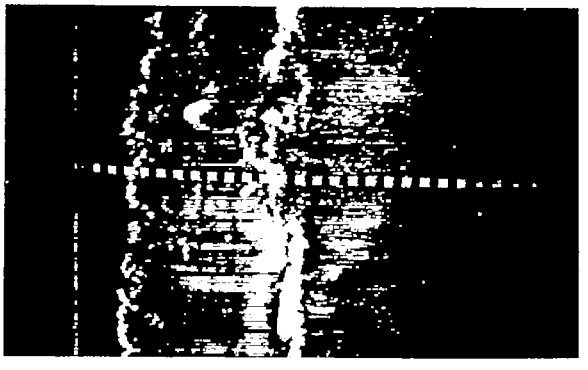

(c) Icing time, 23 minutes.
Drag coefficient, 0.0164.
Lower surface, before ice removal.

C-31293

Figure 21. - Typical heavy glaze-ice formations on airfoil with cyclically de-iced leading-edge section at 2° angle of attack. Airspeed, 260 miles per hour; datum air temperature, 25° F; liquid-water content, 1.4 grams per cubic meter; initial drag coefficient, 0.00835; icing period, approximately 260 seconds; heat-on period, 15 seconds.

2744

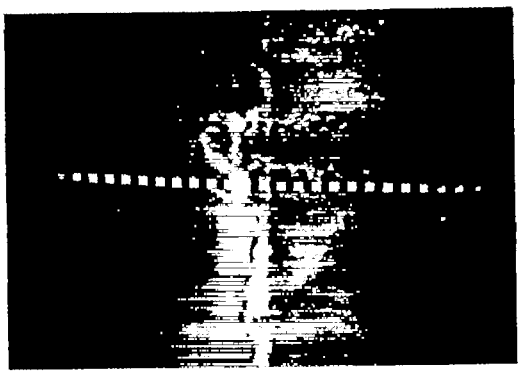

(d) Icing time, $23\frac{1}{2}$ minutes.

Drag coefficient, 0.0114.
Lower surface, after ice removal.

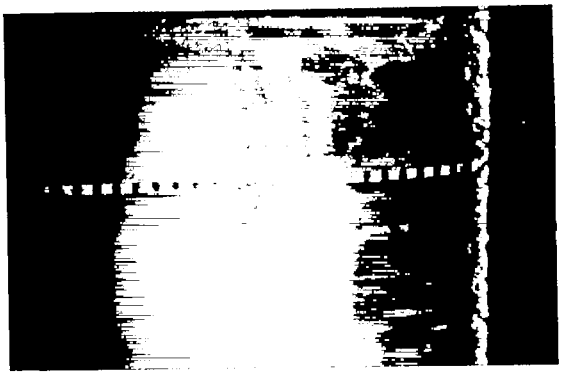

(e) Icing time, $27\frac{1}{2}$ minutes.

Drag coefficient, 0.0159.
Upper surface, before ice removal.

NACA
C-31294

Figure 21. - Concluded. Typical heavy glaze-ice formations on airfoil with cyclically de-iced leading-edge section at 2° angle of attack. Airspeed, 260 miles per hour; datum air temperature, 25° F; liquid-water content, 1.4 grams per cubic meter; initial drag coefficient, 0.00835; icing period, approximately 260 seconds; heat-on period, 15 seconds.

2744

(a) Icing time, 5 minutes.
Drag coefficient, 0.0129.
Before ice removal.

(b) Icing time, 6 minutes.
Drag coefficient, 0.0111.
After ice removal.

(c) Icing time, 16 minutes.
Drag coefficient, 0.0119.
After ice removal.

Figure 22. - Typical glaze-ice formations on lower surface of airfoil with cyclically de-iced leading-edge section at 5° angle of attack. Airspeed, 180 miles per hour; datum air temperature, 23° F; liquid-water content, 1.25 grams per cubic meter; initial drag coefficient, 0.00956; icing period, approximately 260 seconds; heat-on period, 16 seconds.

2744

(a) Icing time, 9 minutes. Drag coefficient, 0.0240. Upper surface, before ice removal.

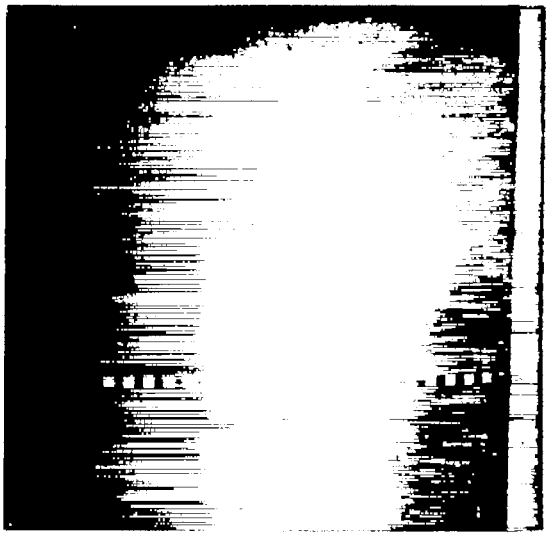

(b) Icing time, 23 minutes. Drag coefficient, 0.0135. Upper surface, after ice removal.

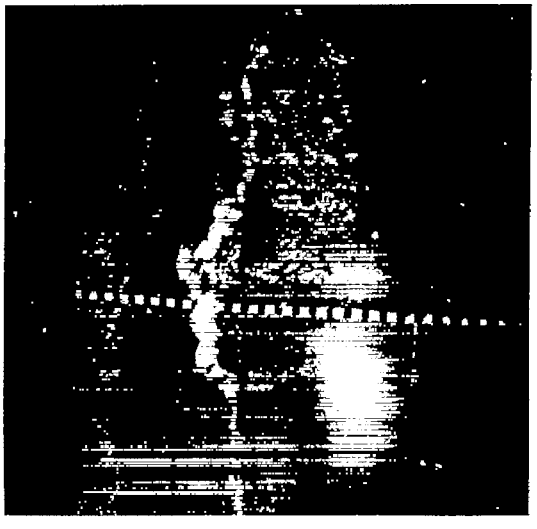

(c) Icing time, 27 minutes. Drag coefficient, 0.0217. Lower surface, before ice removal.

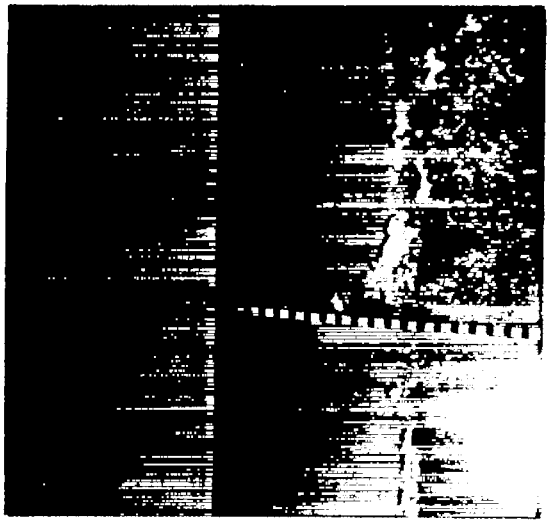

(d) Icing time, $27\frac{1}{2}$ minutes. Drag coefficient, 0.0135. Lower surface, after ice removal.

C-31296

Figure 23. - Typical glaze-ice formations on airfoil with cyclically de-iced leading-edge section at 8° angle of attack. Airspeed, 260 miles per hour; datum air temperature, 25° F; liquid-water content, 1.0 gram per cubic meter; initial drag coefficient, 0.0130; icing period, approximately 260 seconds; heat-on period, 17 seconds.

2744

CH-7

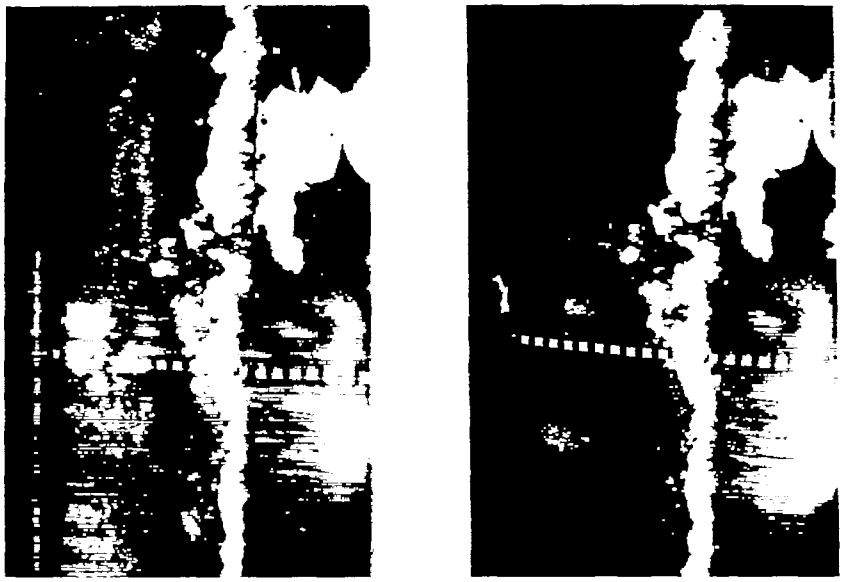

(a) Icing time, 16 minutes. Drag coefficient, 0.0237. Before ice removal.

(b) Icing time, $16\frac{1}{2}$ minutes. Drag coefficient, 0.0153. After ice removal.

C-31297

Figure 24. - Typical heavy ridge-type runback icing on lower surface of airfoil with cyclically de-iced leading-edge section at 8° angle of attack. Airspeed, 180 miles per hour; datum air temperature, 25° F; liquid-water content, 1.25 grams per cubic meter; initial drag coefficient, 0.0121; icing period, approximately 260 seconds; heat-on period, 15 seconds.

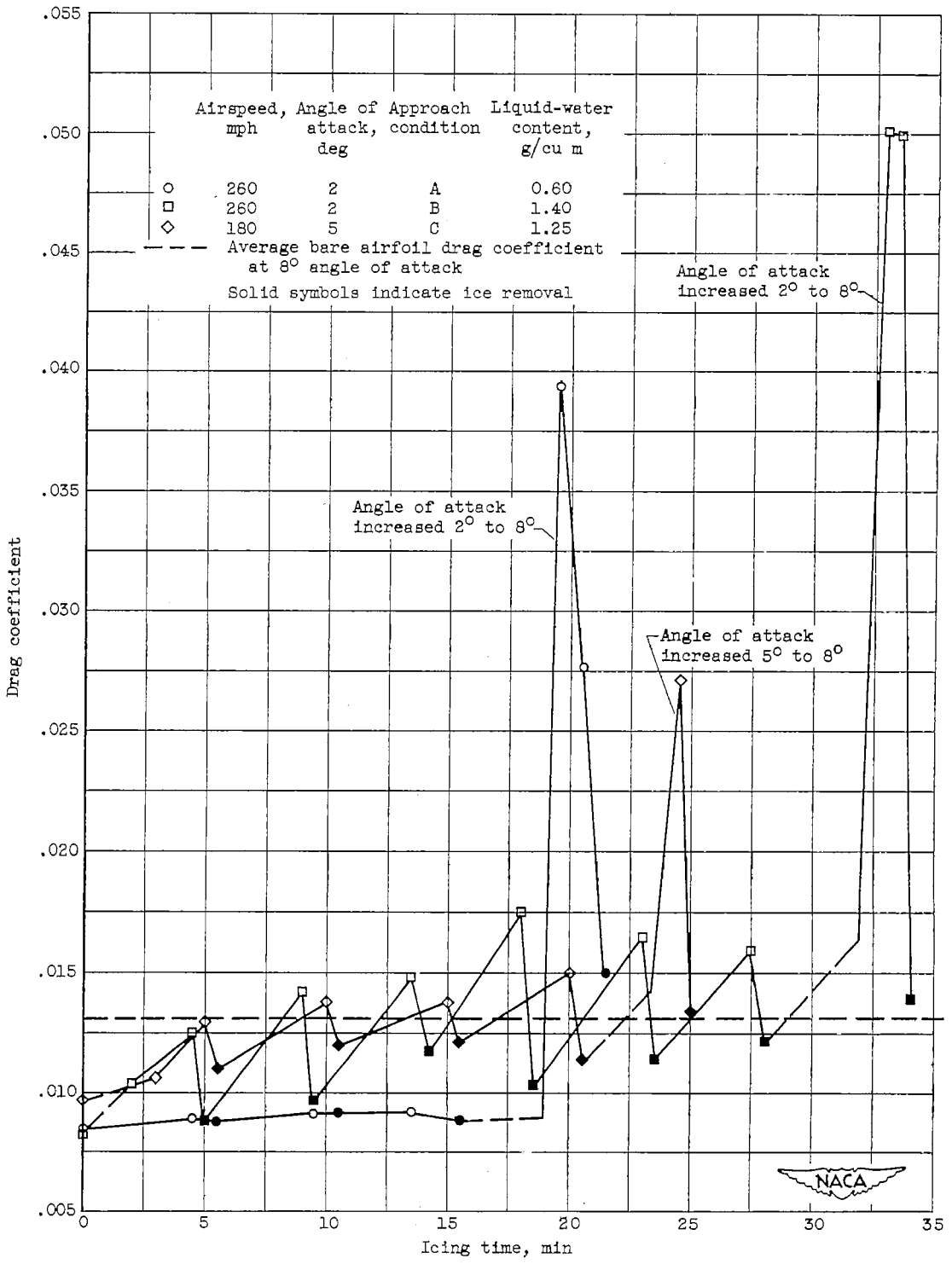

Figure 25. - Drag penalties associated with change in angle of attack (simulating a landing approach condition) during icing period of airfoil with cyclic de-icing system. Datum air temperature, approximately 25° F; icing period, approximately 260 seconds; heat-on period, 15 seconds.

2744

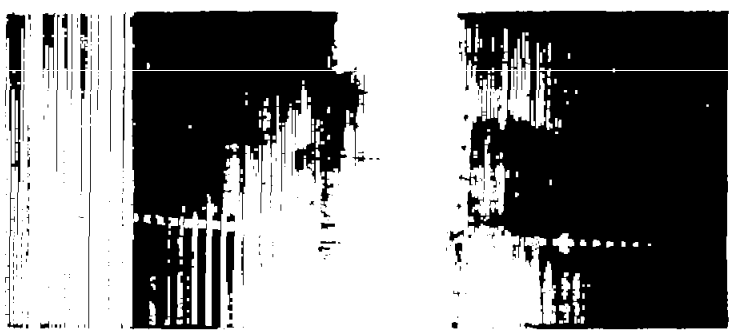

(a) Initial frost deposit on afterbody lower surface after approximately 1 minute in icing condition.

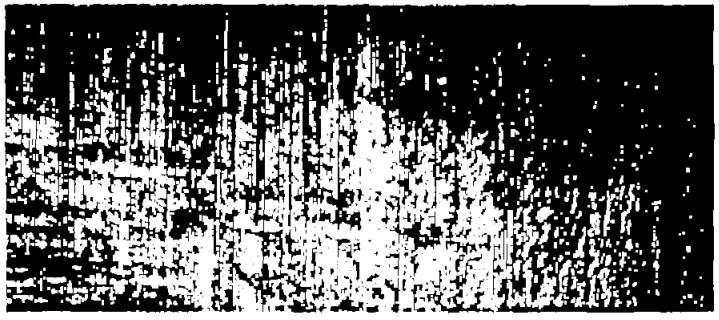

(d) Large frost feathers and formations protruding into air stream after approximately 1 hour in heavy icing condition.

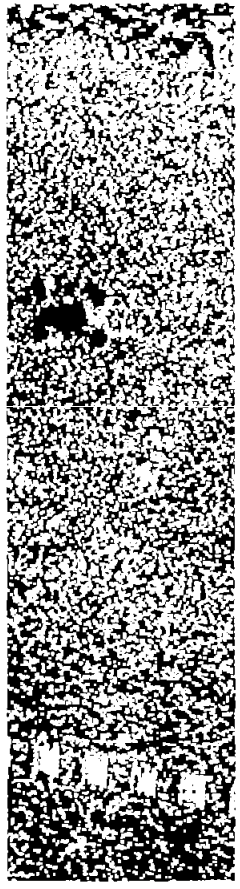

(b) Frost pinnacles caused by direct water impingement on initial frost deposit.

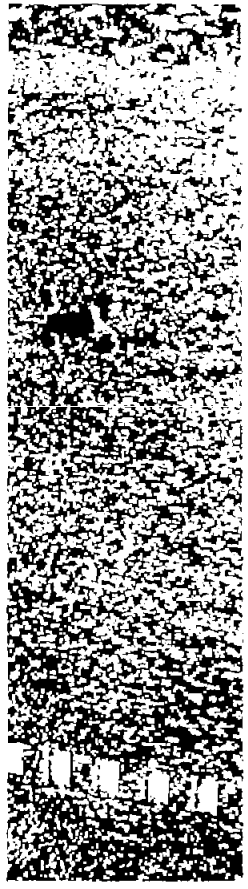

(c) Growth of frost pinnacles into air stream due to droplet impingement.

NACA

C-31298

Figure 26. - Typical frost formation and growth on airfoil afterbody.

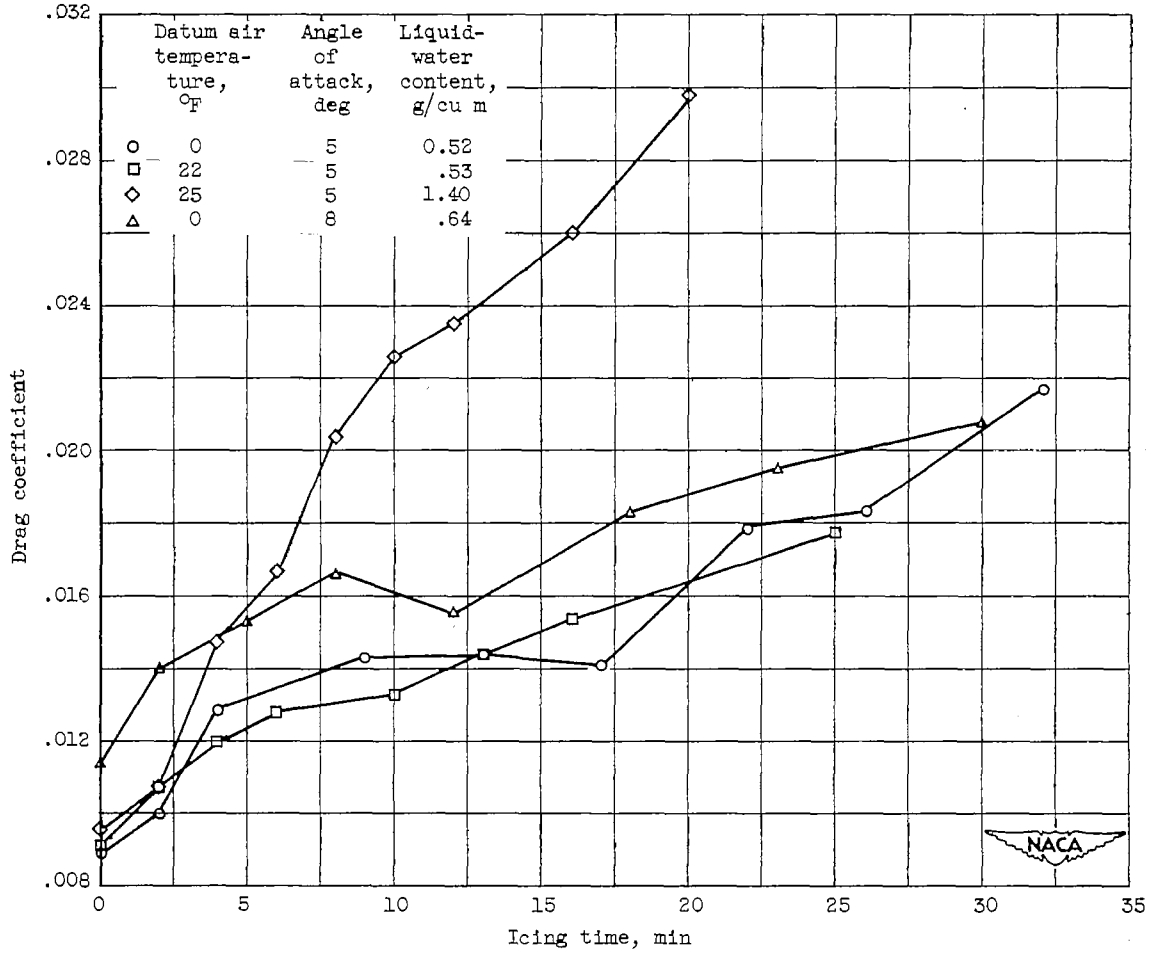

Figure 27. - Drag coefficients associated with combination of leading-edge ice formations and afterbody frost formations as function of time in icing. Airspeed, 180 miles per hour.

2744

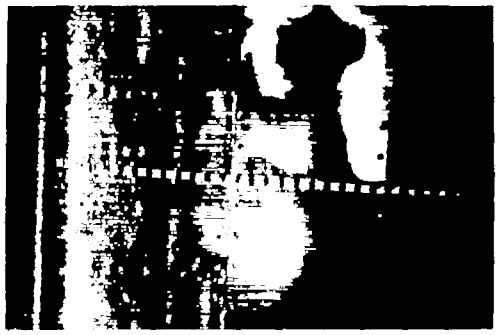

(a) Icing time, 4 minutes. Drag coefficient, 0.0148. Leading-edge lower surface.

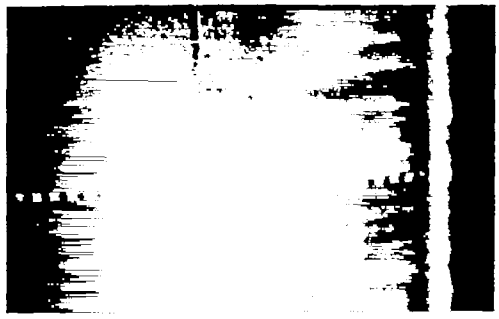

(b) Icing time, 8 minutes. Drag coefficient, 0.0204. Leading-edge upper surface.

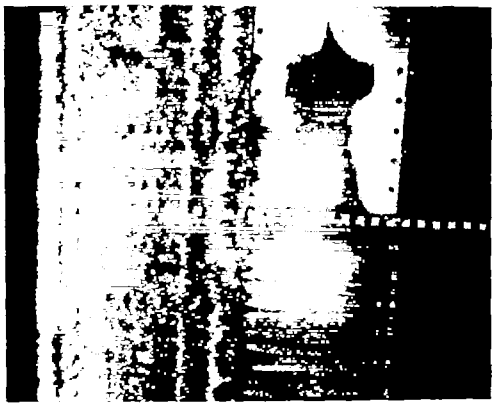

(c) Icing time, 10 minutes. Drag coefficient, 0.0226. Leading-edge lower surface.

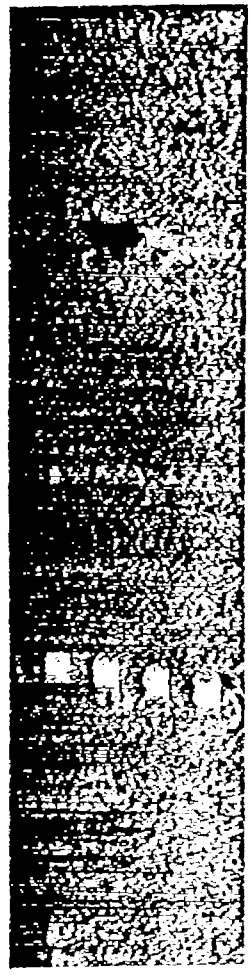

(d) Icing time, 12 minutes. Drag coefficient, 0.0235. Lower-surface frost on compartment 2.

C-31299

Figure 28. - Typical glaze-ice and frost formations with high rate of water catch on unheated airfoil at 5° angle of attack. Airspeed, 180 miles per hour; datum air temperature, 25° F; liquid-water content, 1.4 grams per cubic meter; initial drag coefficient, 0.00958.

(a) Icing time, 4 minutes. Drag coefficient, 0.0120. Leading-edge lower surface.

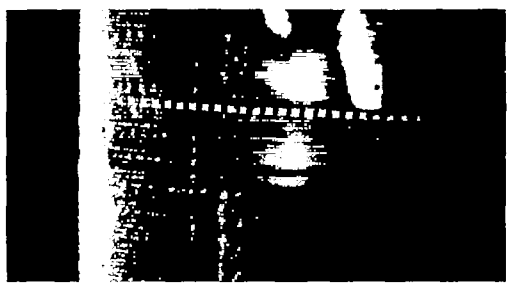

(b) Icing time, 10 minutes. Drag coefficient, 0.0133. Leading-edge lower surface.

(c) Icing time, 13 minutes. Drag coefficient, 0.0144. Leading-edge upper surface.

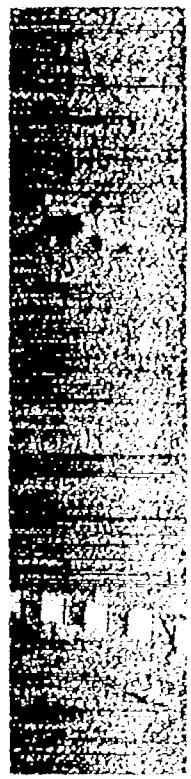

(d) Icing time, 16 minutes. Drag coefficient, 0.0154. Lower-surface frost on compartment 2.

NACA C-31300

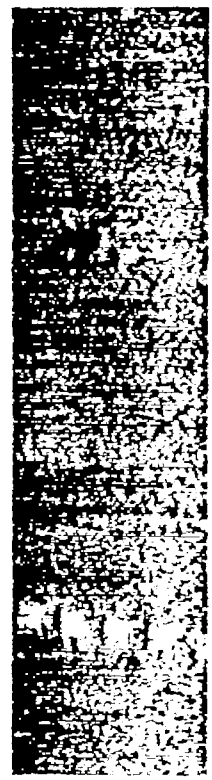

(e) Icing time, 25 minutes. Drag coefficient, 0.0178. Lower-surface frost on compartment 2.

2744

Figure 29. - Typical ice and frost formations with low rate of water catch on unheated airfoil at 5° angle of attack. Airspeed, 180 miles per hour; datum air temperature, 22° F; liquid-water content, 0.53 gram per cubic meter; initial drag coefficient, 0.00911.

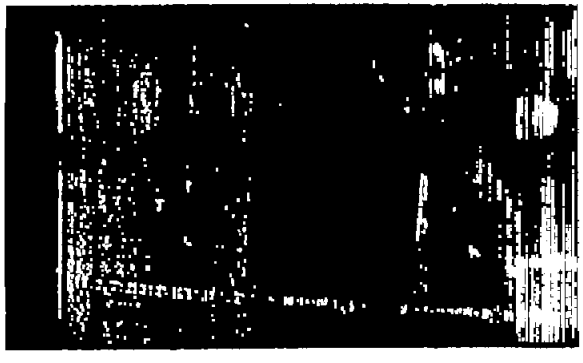

(a) Icing time, 8 minutes. Drag coefficient, 0.0166. Leading-edge ice.

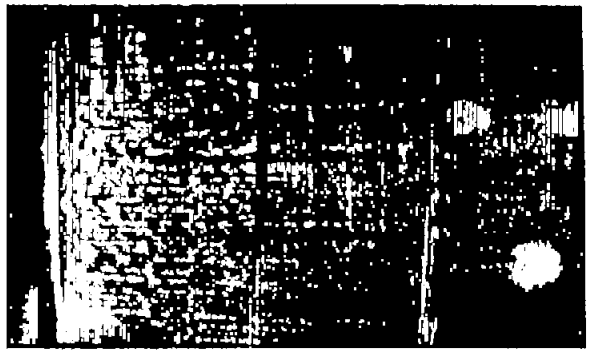

(b) Icing time, 21 minutes. Drag coefficient, 0.0187. Leading-edge ice.

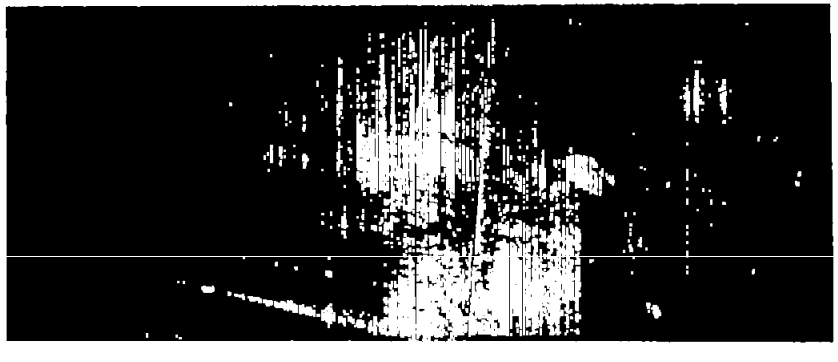

E-31301

(c) Icing time, 23 minutes. Drag coefficient, 0.0195. Frost formations on afterbody.

Figure 30. - Rime-ice and frost formations on lower surface of unheated airfoil at 8° angle of attack. Airspeed, 180 miles per hour; datum air temperature, 0° F; liquid-water content, 0.64 gram per cubic meter; initial drag coefficient, 0.0114.

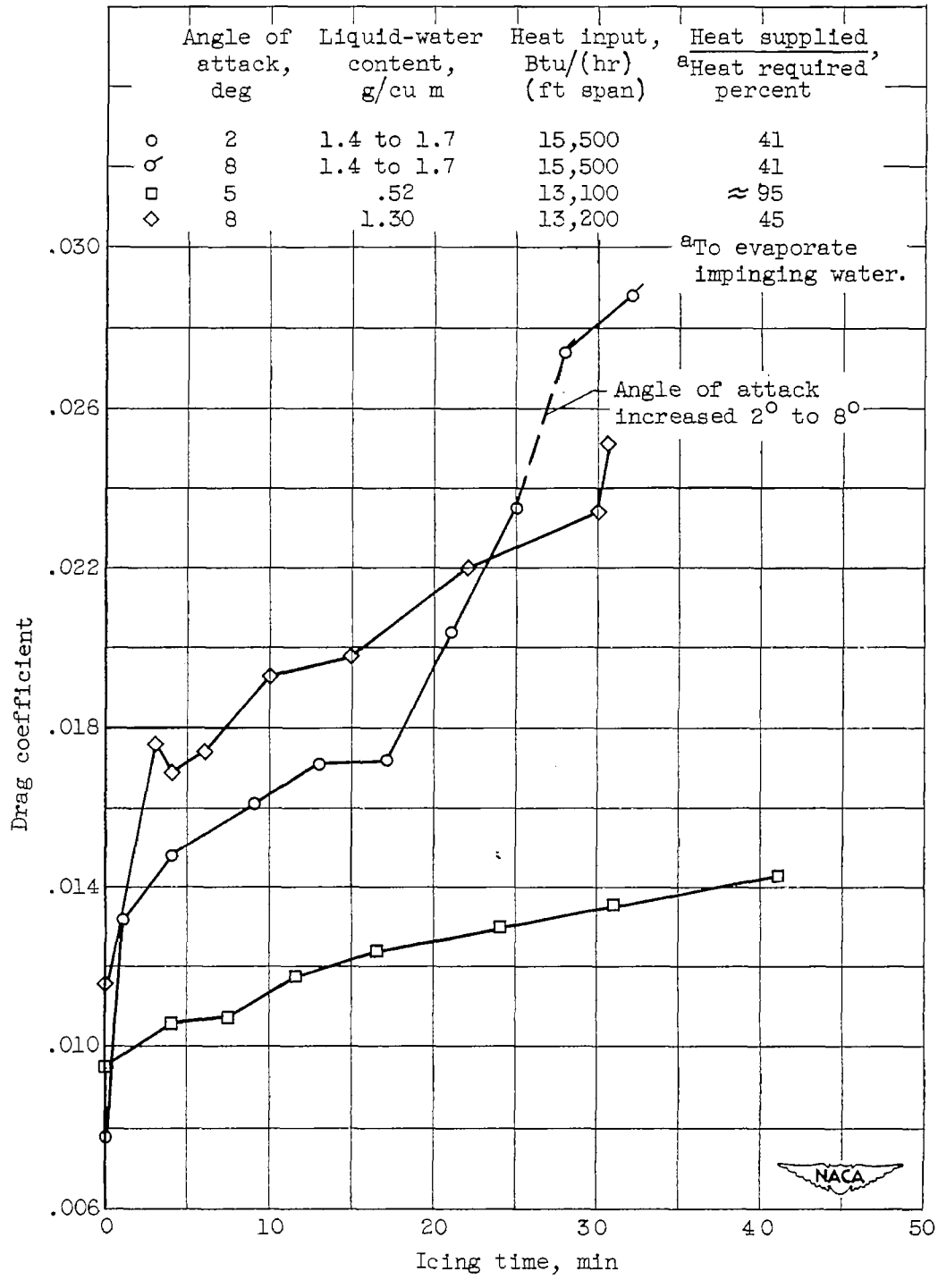

Figure 31. - Variation of drag caused by afterbody frost formations and runback icing as function of time in icing with leading edge continuously heated. Airspeed, 180 miles per hour; datum air temperature, 0° F.

(a) Icing time, 13 minutes. Drag coefficient, 0.0171. Leading-edge lower surface.

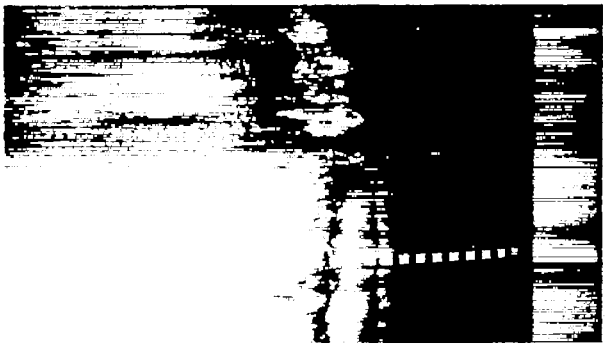

(b) Icing time, 17 minutes. Drag coefficient, 0.0172. Leading-edge upper surface.

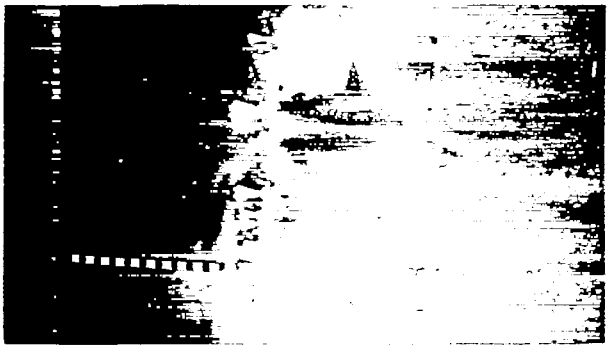

(c) Icing time, 21 minutes. Drag coefficient, 0.0204. Leading-edge lower surface.

NACA
C-31302

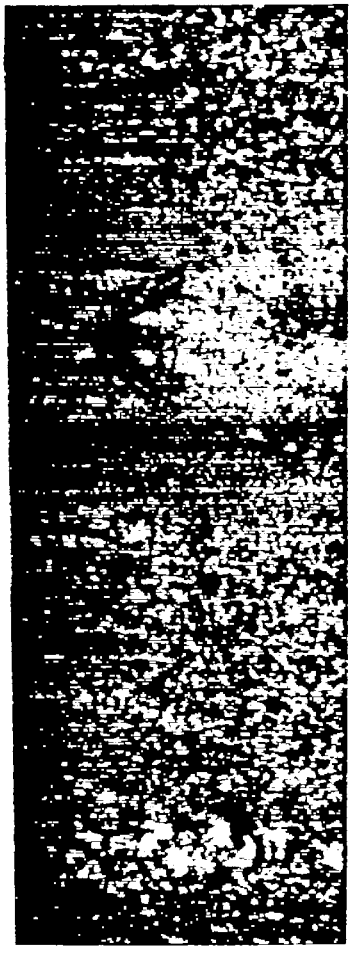

(d) Icing time, 21 minutes. Lower-surface frost on compartment 3.

Figure 32. - Combination runback icing and afterbody frost formations on airfoil at 2° angle of attack. Airspeed, 180 miles per hour; datum air temperature, 0° F; liquid-water content, approximately 1.5 grams per cubic meter; initial drag coefficient, 0.00785; leading edge continuously heated.

(a) Icing time, 15 minutes. Drag coefficient, 0.0198. Leading-edge lower surface.

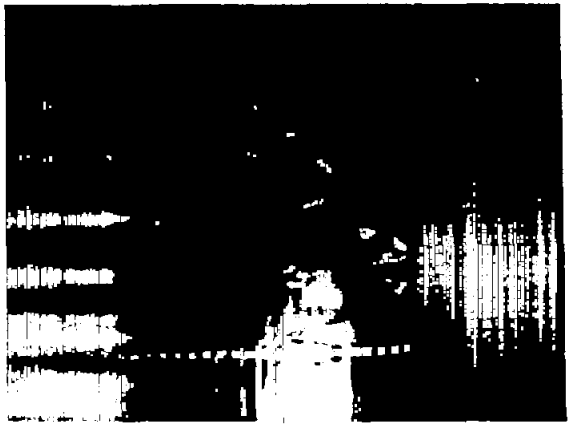

(c) Icing time, $30\frac{1}{2}$ minutes. Drag coefficient, 0.0251. Leading-edge upper surface.

(b) Icing time, 15 minutes. Lower surface frost on compartment 2.

C-31303

(d) Icing time, $30\frac{1}{2}$ minutes. Lower-surface frost on compartment 2.

Figure 33. - Runback icing and frost formations on airfoil with leading-edge section continuously heated at 8° angle of attack. Airspeed, 180 miles per hour; datum air temperature, 0° F; liquid-water content, 1.3 grams per cubic meter; initial drag coefficient, 0.0115.

2744

CH-8 back

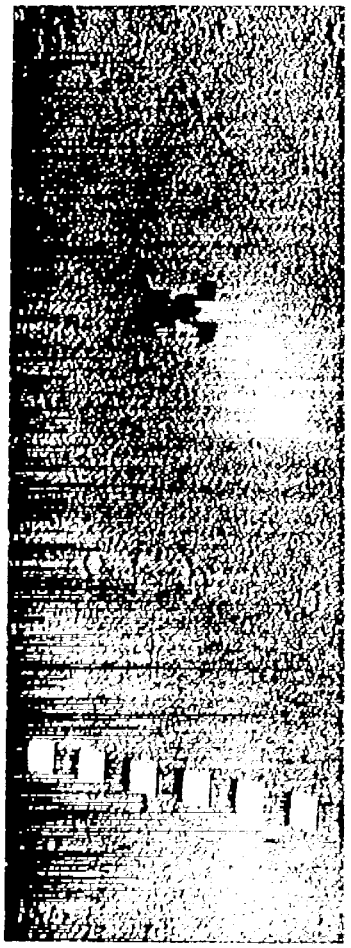

(a) Icing time, $7\frac{1}{2}$ minutes. Drag coefficient, 0.0107. Lower-surface frost on compartment 2.

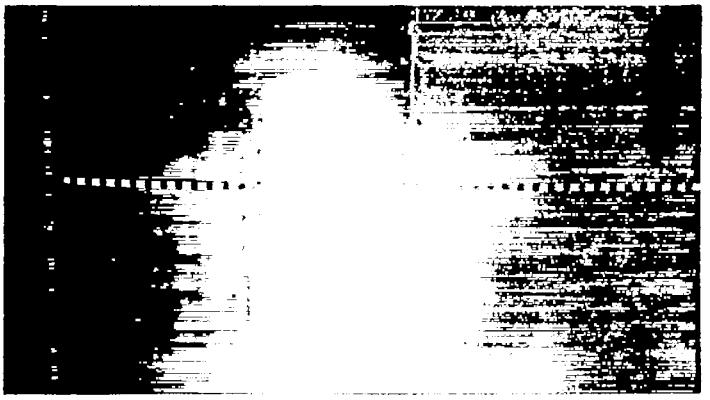

(b) Icing time, 24 minutes. Drag coefficient, 0.0130. Leading-edge lower surface.

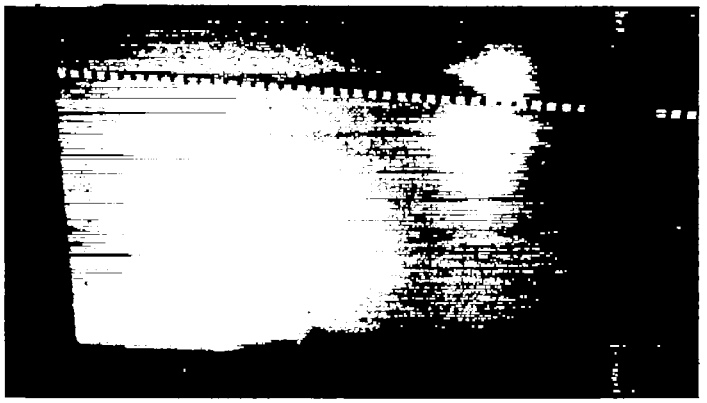

(c) Icing time, 31 minutes. Drag coefficient, 0.0136. Upper-surface frost on compartments 3 and 4.

C-31304

Figure 34. - Frost formations on airfoil at 5° angle of attack. Airspeed, 180 miles per hour; datum air temperature, 0° F; liquid-water content, 0.52 gram per cubic meter; initial drag coefficient, 0.00950.

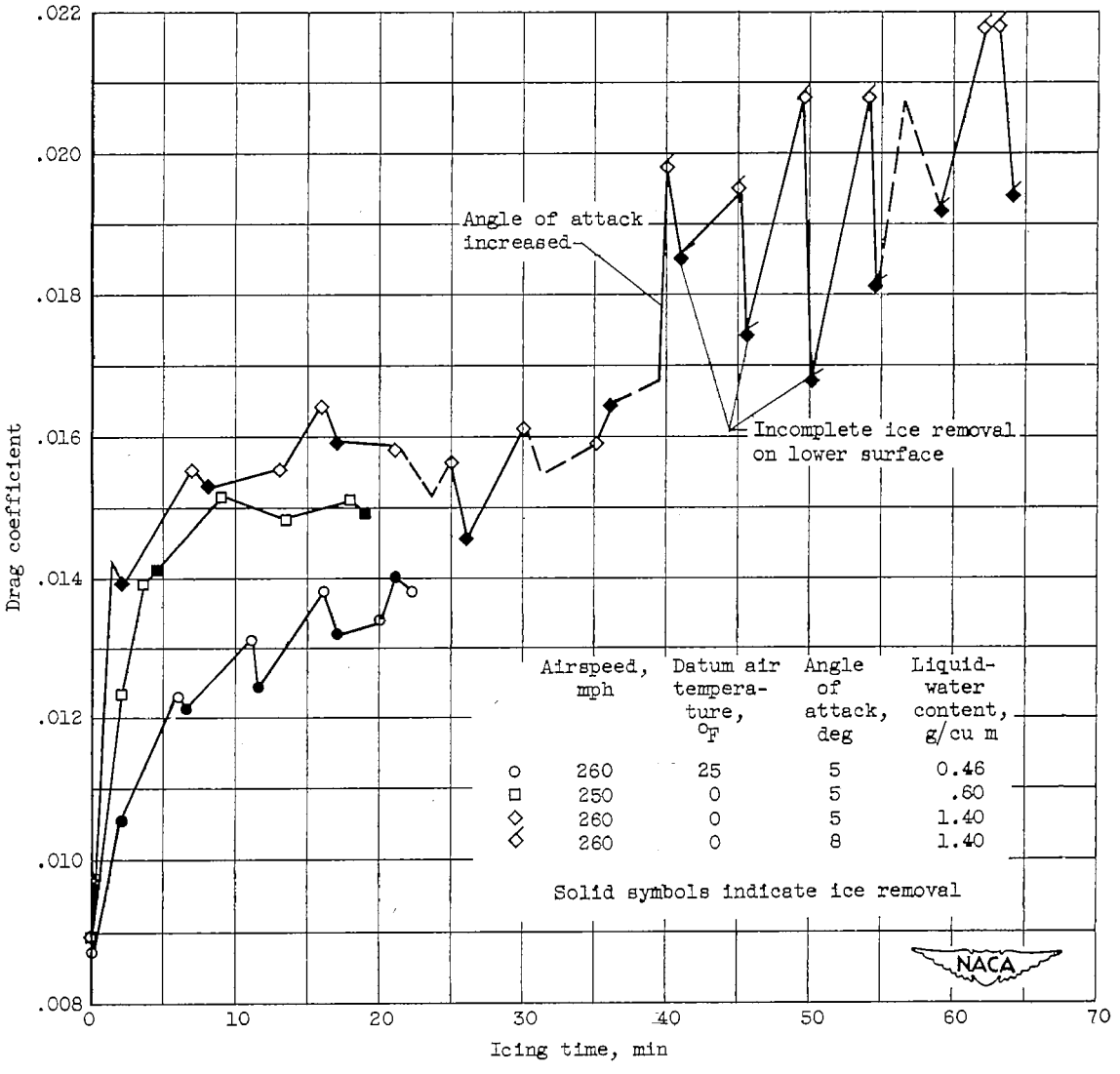

Figure 35. - Drag coefficients associated with cyclically de-iced airfoil leading-edge section and frosted afterbody as function of time in icing.

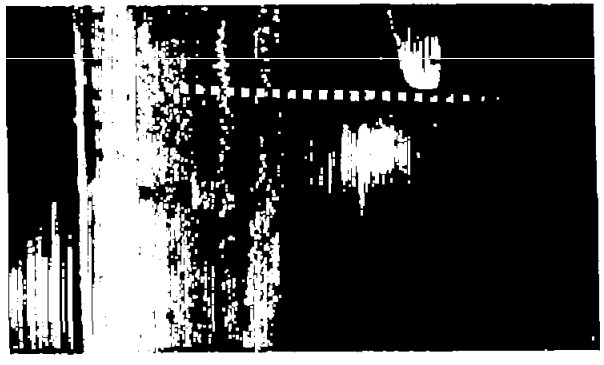

(a) Icing time, 7 minutes. Drag coefficient, 0.0155. Lower surface, before ice removal.

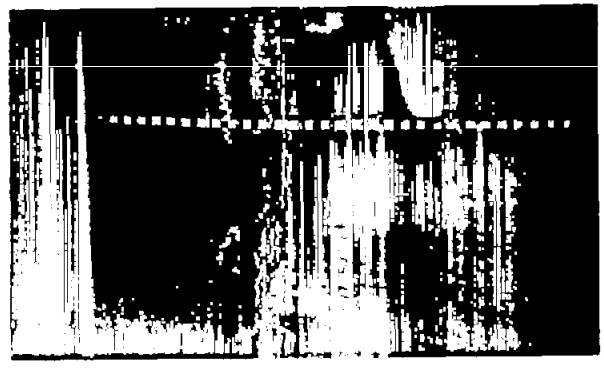

(b) Icing time, 8 minutes. Drag coefficient, 0.0153. Lower surface, after ice removal.

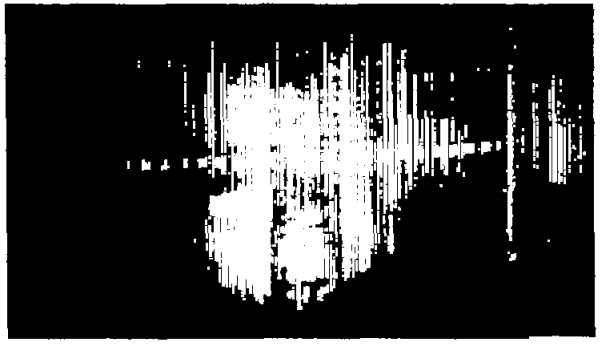

(c) Icing time, 25 minutes. Drag coefficient, 0.0156. Upper surface, before ice removal.

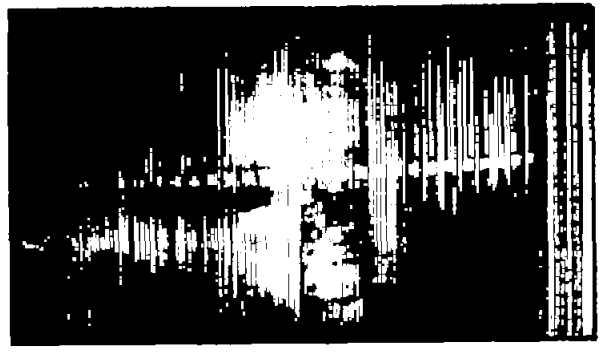

(d) Icing time, 26 minutes. Drag coefficient, 0.0145. Upper surface, after ice removal.

C-31305

Figure 36. - Cyclically de-iced leading-edge and afterbody frost formations for airfoil at 5° angle of attack. Airspeed, 260 miles per hour; datum air temperature, 0° F; liquid-water content, 1.4 grams per cubic meter; initial drag coefficient, 0.00886; icing period, approximately 260 seconds; heat-on time, 18 seconds.

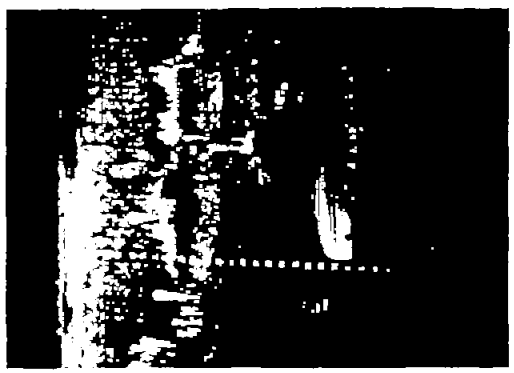

(a) Total time in icing, 45 minutes. Drag coefficient, 0.0195. Leading-edge lower surface, before ice removal.

(b) Total time in icing, $45\frac{1}{2}$ minutes. Drag coefficient, 0.0174. Leading-edge lower surface, after ice removal.

NACA

C-31306

(c) Total time in icing, 54 minutes. Drag coefficient, 0.0208. Leading-edge lower surface, before ice removal.

Figure 37. - Cyclically de-iced leading-edge and afterbody frost formations for airfoil at 8° angle of attack following 40 minutes in icing condition at 5° angle of attack. Airspeed, 260 miles per hour; datum air temperature, 0° F; liquid-water content, 1.4 grams per cubic meter; initial drag coefficient, 0.00886; icing period, approximately 260 seconds.

2744

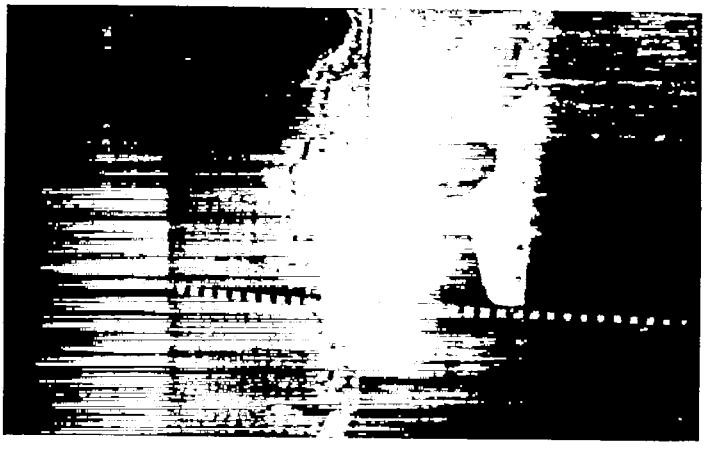

(d) Total time in icing, $54\frac{1}{2}$ minutes. Drag coefficient, 0.0181. Leading-edge lower surface, after ice removal. Heat-on time, 25 seconds.

(e) Total time in icing, 64 minutes. Drag coefficient, 0.0194. Leading-edge upper surface, after ice removal. Heat-on time, 25 seconds.

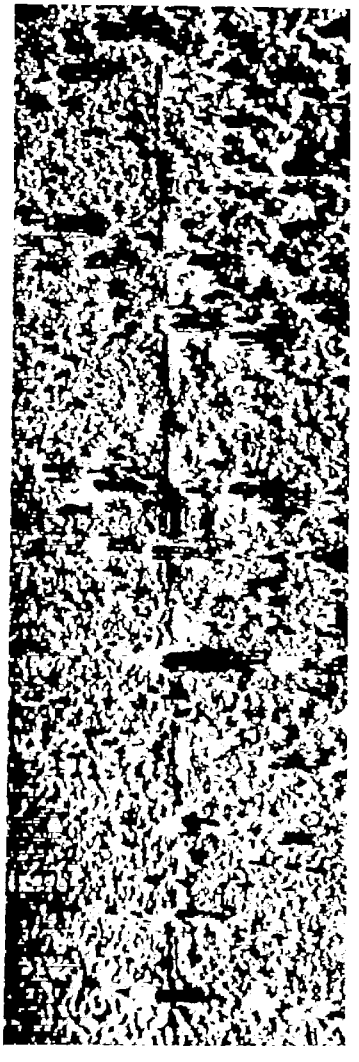

(f) Total time in icing, 64 minutes. Lower-surface frost on compartment 2.

C-31307

Figure 37. - Concluded. Cyclically de-iced leading-edge and afterbody frost formation for airfoil at 8° angle of attack following 40 minutes in icing condition at 5° angle of attack. Airspeed, 260 miles per hour; datum air temperature, 0° F; liquid-water content, 1.4 grams per cubic meter; initial drag coefficient, 0.00886; icing period, approximately 260 seconds.

2744

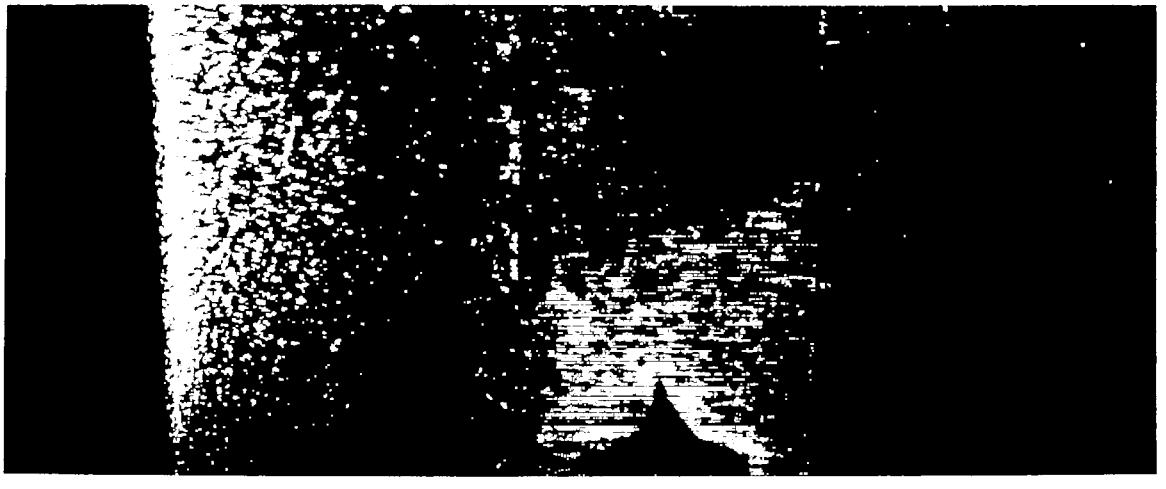

C-31308

Figure 38. - Typical sublimation frost formation on lower surface of airfoil. Airspeed, approximately 100 miles per hour; datum air temperature, -25° to -8° F; angle of attack, 8°; time in frosting condition, 5 minutes.

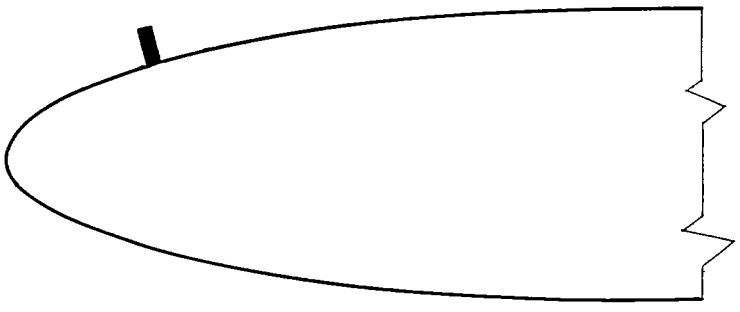

(a) Spoiler protuberance extending full span of airfoil model.

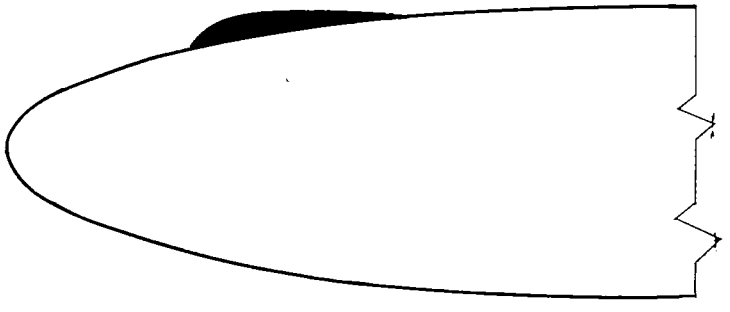

(b) Faired protuberance approximating small half-airfoil section.

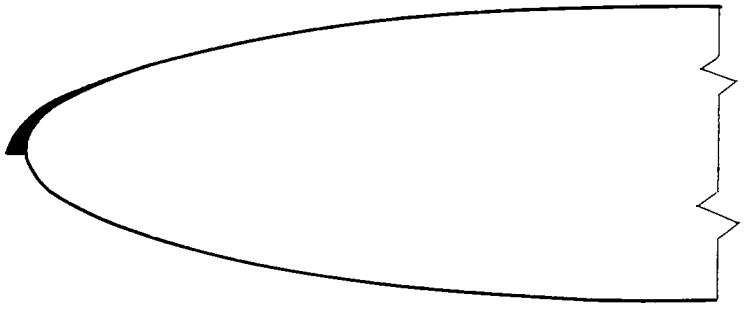

(c) Modified spoiler protuberance with faired trailing section.

Figure 39. - Sketch of protuberance types used in reference 4 to determine airfoil section characteristics.

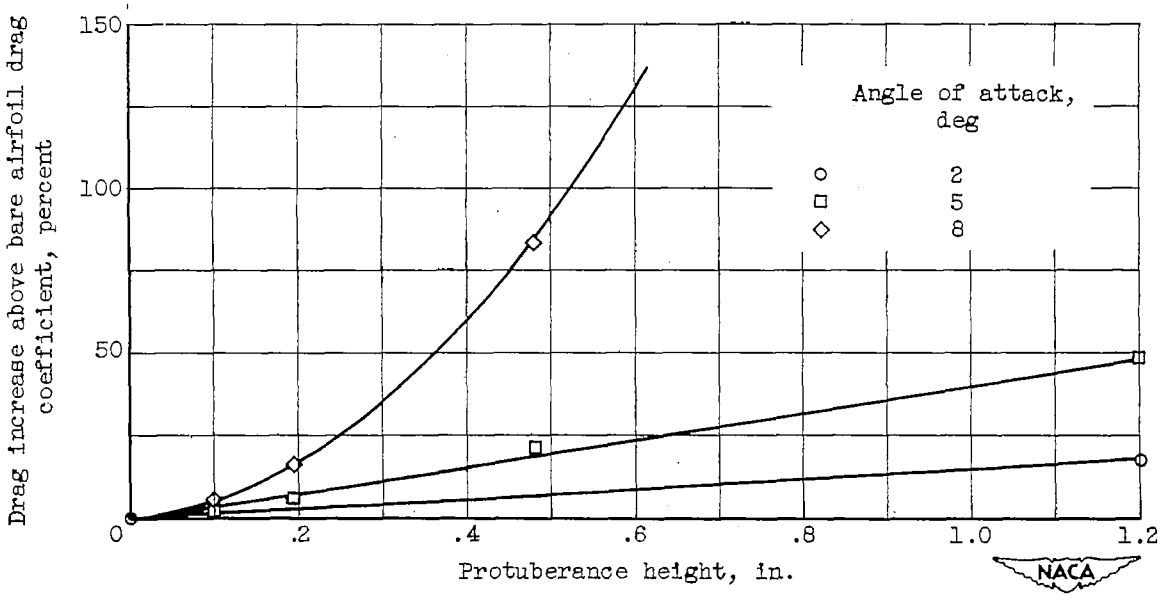

(a) Protuberance location, 0-percent-chord station.

Figure 40. - Percentage drag increase with protuberance height for several angles of attack at three chord stations (ref. 4). (Spoiler protuberance, fig. 39(a).)

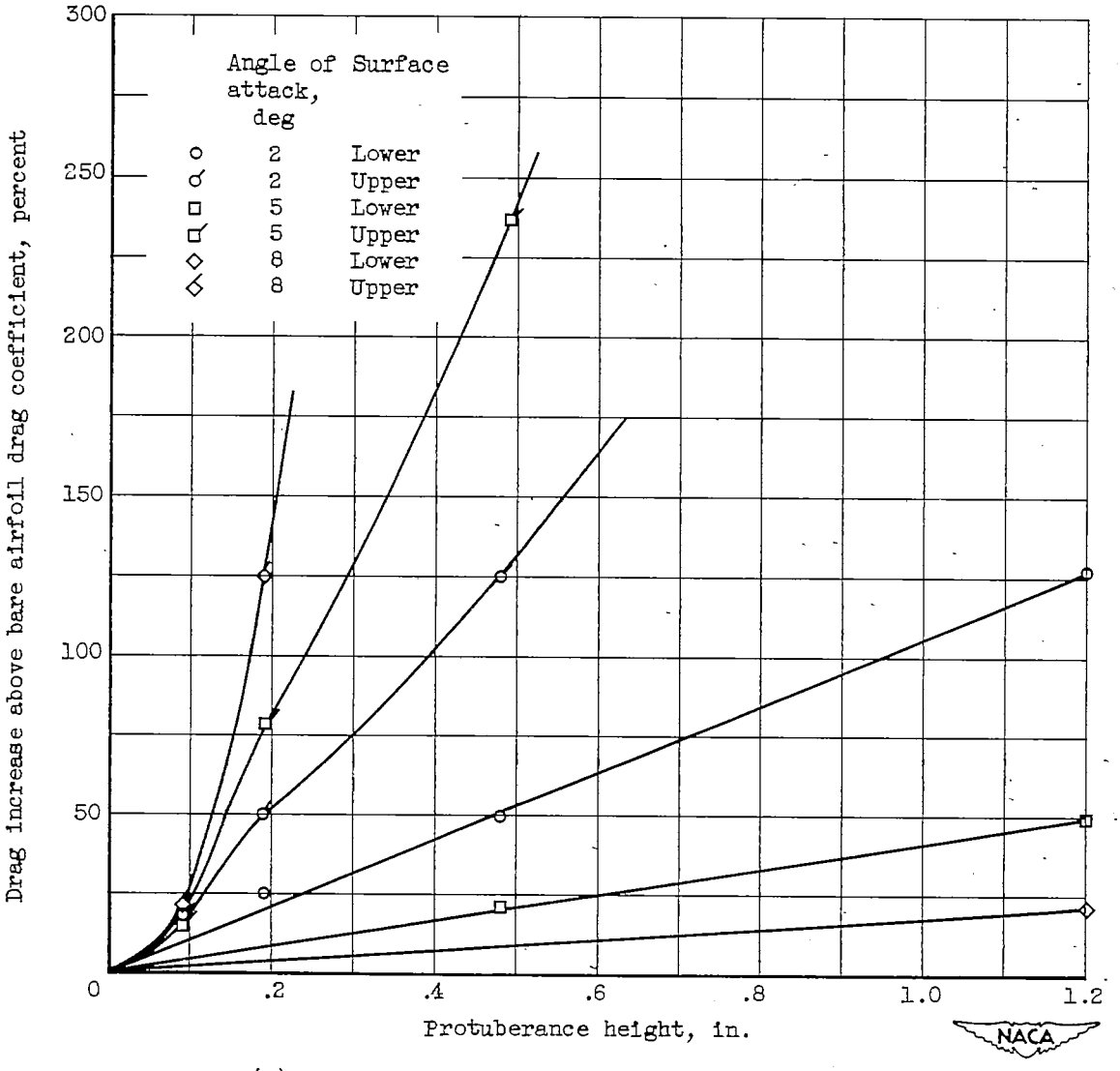

(b) Protuberance location, 5-percent-chord station.

Figure 40. - Continued. Percentage drag increase with protuberance height for several angles of attack at three chord stations (ref. 4). (Spoiler protuberance, fig. 39(a).)

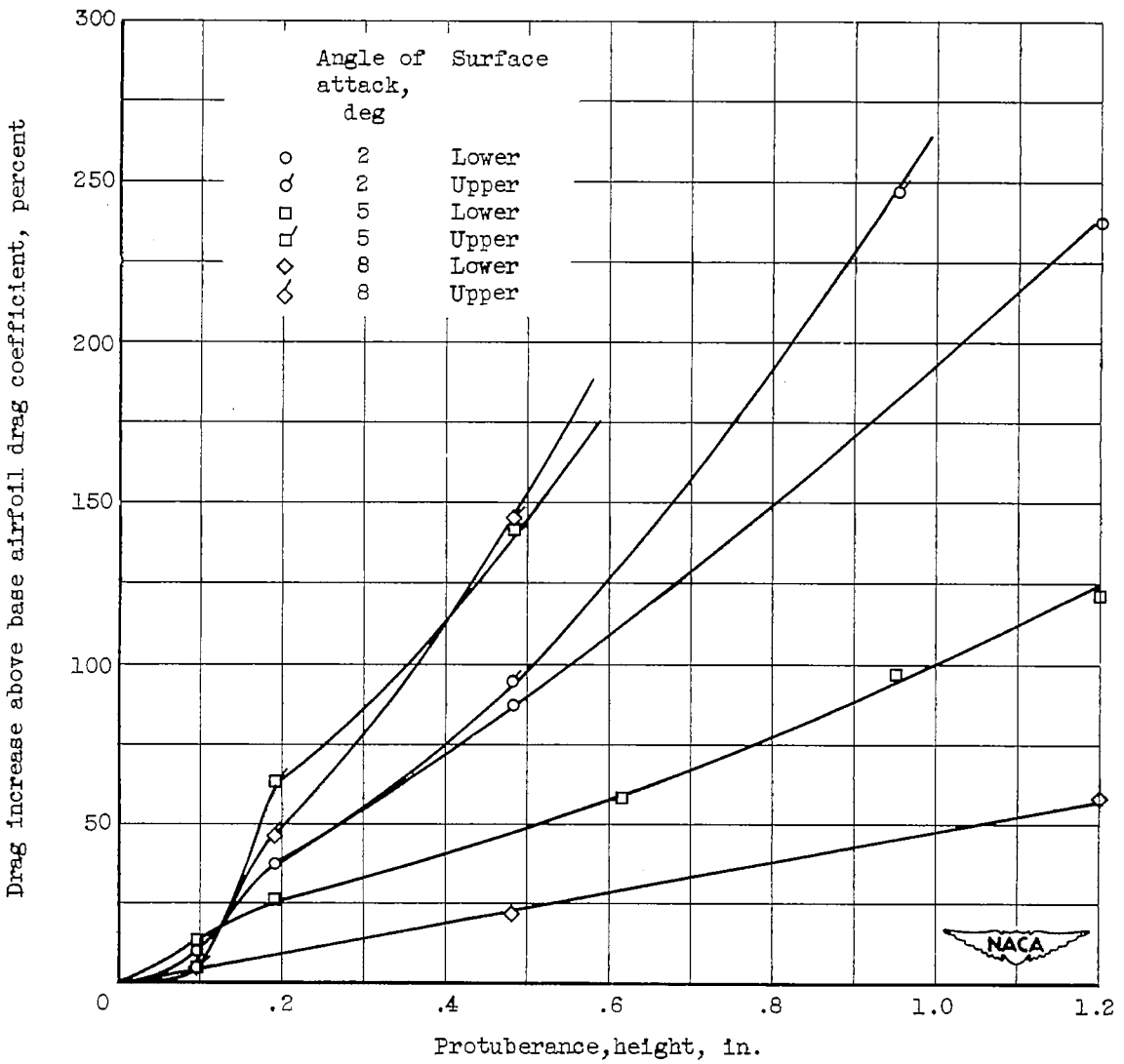

(c) Protuberance location, 15-percent-chord station.

Figure 40. - Concluded. Percentage drag increase with protuberance height for several angles of attack at three chord stations (ref. 4). (Spoiler protuberance, fig. 39(a).)

NACA-Langley - 6-26-53 - 1000